Aus der Abteilung Neurogenetik
(Prof. K.-A. Nave, Ph.D.)
des Max-Planck-Instituts für Experimentelle Medizin
in Göttingen

Experimental therapy with progesterone on a mouse model for hereditary neuropathy with liability to pressure palsies (HNPP)

INAUGURAL-DISSERTATION
zur Erlangung des Doktorgrades

der Medizinischen Fakultät der
Georg-August-Universität zu Göttingen

vorgelegt von
Heidi Granat
aus
Espoo (Finnland)

Göttingen 2019

Dekan:	Prof. Dr. rer. nat. H. K. Kroemer
Referent:	Prof. Dr. med. M. W. Sereda
Ko-Referent / in:	Prof. Dr. M. Müller
Datum der mündlichen Prüfung:	10.03.2020

Hiermit erkläre ich, die Dissertation mit dem Titel “Experimental therapy with progesterone on a mouse model for hereditary neuropathy with liability to pressure palsies (HNPP)” eigenständig angefertigt und keine anderen als die von mir angegebenen Quellen und Hilfsmittel verwendet zu haben.

Espoo, den 05. 05. 2019 ……...

Table of contents

Index of figures

Abbreviations

Aq. dest.	distilled water
bp	base-pair
CB	conduction block
cDNA	complementary DNA
CNS	central nervous system
CMAP	compound muscle action potential
CMT	Charcot-Marie-Tooth disease
Ct	threshold cycle
ddH_2O	double-distilled water
DDSA	duodecenyl succinic anhydride
DML	distal motor latency
DNA	deoxyribonucleic acid
dNTP	deoxyribonucleotide triphosphate
EDTA	ethylendiamidtetraacetic acid
EtOH	ethanol
g	gram
h	hour
HNPP	hereditary neuropathy with liability to pressure palsies
kb	kilobase

kDa	kilodalton
M	molar
MGB	modified Gitschier buffer
min	minute
MNA	methyl nacid anhydride
mRNA	messenger RNA
m/s	meter per second
mV	millivolt
N.	nervus
ng	nanogram
NRG1	neuregulin-1
p	p-value
P	postnatal day
PAK1	p21-activated kinase
PCR	polymerase chain reaction
pg	picogram
PKA	proteinkinase A
PKC	proteinkinase C
PMP22	peripheral myelin protein 22
PNS	peripheral nervous system

PR	progesterone receptor
PRE	progesterone response elements
RNA	ribonucleic acid
rRNA	ribosomal RNA
rpm	revolutions per minute
RT	room temperature
RT-PCR	reverse transcription polymerase chain reaction
s	second
TAE	tris-acetate-EDTA
TH-Progesterone	3α-, 5α-tetrahydroprogesterone
Tris	tris(hydroxymethyl)aminomethane
V	volt

1. Introduction

The nervous system, a network of neurons and neuroglia, coordinates the voluntary and involuntary actions of an animal, transmits signals to and from different parts of its body, and allows communication with its environment. In vertebrates it is divided in a central nervous system (CNS) and a peripheral nervous system (PNS). The CNS contains the brain and the spinal cord, whereas the PNS consists of nerves and ganglia that connect the CNS to the rest of the body.

Nerve cells, also known as neurons, are specialized cells in the body as they can communicate with each other in a process called neurotransmission. The process involves an electrical signal or axon potential that results in the release of chemicals or neurotransmitters at the contact point between the cells, known as the synapse. A nerve cell that receives a synaptic signal may be excited, inhibited, or otherwise modulated.

Glial cells, i.e. astrocytes, oligodendrocytes and microglia in the CNS, and Schwann cells in the PNS, provide structural and metabolic support for neuronal networks. Oligodendrocytes and Schwann cells generate a lipid-rich wrapping called myelin around axons, providing electrical insulation which allows high speed transmission of electrical signals. Oligodendrocytes can wrap around several axons and myelinate them, whereas Schwann cells provide insulation to only one axon. Action potentials arise when the neuronal membrane potential reaches a threshold level that changes the permeability of the nerve cell´s axonal membranes to specific ions. Action potential generation occurs at specific gaps in the myelin wrapping, called nodes of Ranvier, allowing saltatory propagation with reprogation at the nodes. This arrangement greatly enhances the velocity of action potential conduction. Not surprisingly, loss of myelin, or alterations in its structure, as occurs in many diseases, can cause a variety of neurological defects.

This thesis focuses on hereditary neuropathy with liability to pressure palsies (HNPP), a demyelinating disease characterized by recurrent painless focal neuropathies. At the genomic level HNPP patients present a loss of the peripheral myelin protein 22 gene (*PMP22*). Treatment of the disease is symptomatic. In this thesis the phenotype of a transgenic mouse model for HNPP was reviewed and compared to that of human HNPP patients and an experimental therapy study with progesterone was performed on these animals.

1.1. HNPP and its prevalence

Charcot-Marie-Tooth disease (CMT), also known as hereditary motor and sensory neuropathy (HMSN), is a heterogenous group of hereditary neuropathies with a population prevalence of 1:2500 (Rossor et al. 2016), placing CMT among the most common inherited diseases (Emery 1991). Within the CMT diseases, hereditary neuropathy with liability to pressure palsies (HNPP) is an autosomal dominant disorder characterized by episodic, recurrent peripheral sensory and motor neuropathies (Chance et al. 1993) in a single nerve (mononeuropathy). Males and females are equally affected by HNPP (Bird 2014). This demyelinating disease, first described by de Jong in 1947 (De Jong 1947), is inherited with high penetrance but variable expression (Pareyson et al. 1996). The prevalence of HNPP is unknown, however, a population study from Finland gives an estimate of 16/100.000 (Meretoja et al. 1997). Nevertheless, a possible lack of symptoms in patients can lead to an underestimation of the disease prevalence (Kramer et al. 2016).

1.2. Clinical features of HNPP

The onset of symptoms in patients with HNPP is typically in the second or third decade, although the first episode occasionally occurs in childhood (Pareyson et al. 1996). Painless nerve palsies and sensory loss characteristic for the neuropathy are often triggered by minor traumas or compression in various locations (De Jong 1947; Davies 1954; Earl et al. 1964; Staal et al. 1965), such as the brachial plexus, peroneal, ulnar, radial or median nerves (Cho et al. 2014), or provoked by physical activity, including repetitive motions or stretching of the affected limb (Li et al. 2004). The clinical symptoms of an undiagnosed HNPP can also be manifested after a surgical procedure (Kramer et al. 2016). Carpal tunnel syndrome can occur when the median nerve at the wrist is affected, and entrapment of the peroneal nerve at the fibular head can cause a foot drop (Del Colle et al. 2003). Pes cavus and hammertoes have been described in more severe cases (Amato et al. 1996), as have hypo- and areflexia (Pareyson et al. 1996). Pain is rarely reported as a symptom but may be an initial or a chronic manifestation of the disease (de Oliveira et al. 2016). The clinical progression and severity of HNPP is highly various (Windebank 1993). The symptoms are brief and improve generally within days, weeks or months (Pareyson et al. 1996), with full recovery occurring in 50 % of episodes. Remaining symptoms are rarely severe (Bird 2014). However, the development of a chronic peripheral neuropathy is possible in

specific cases (Windebank 1993). Approximately 10-15 % of HNPP patients remain clinically asymptomatic (Gouider et al. 1995; Lenssen et al. 1998).

The affected limbs usually show significant slowing and conduction blocks in nerve conduction velocity (NCV) studies, especially across common pressure sites. Distal motor latencies (DML) are increased, in particular of the median and peroneal nerves (Behse et al. 1972a; Amato et al. 1996; Hong et al. 2003). In addition, sensory nerve conduction velocities are often decreased and sensory nerve action potential amplitudes are reduced (Li et al. 2002; Hong et al. 2003). It is hypothesized that the focal symptoms of HNPP are caused by a reversible conduction block (CB), defined by > 50 % reduction of compound muscle action potential (CMAP) amplitudes between proximal and distal sites of stimulation (Li et al. 2004; van Paassen et al. 2014). The presence of CB indicates a failure of axon potential propagation at a given site along a structurally intact axon and is consistent with a myelinopathy (Lawson and Arnold 2014).

1.3. Molecular genetics of HNPP

HNPP is mostly caused by a heterozygous 1.5 Mb deletion on chromosome 17p11.2 that includes the peripheral myelin protein 22 (*PMP22*) gene (Chance et al. 1993). The same gene region is duplicated in Charcot-Marie-Tooth disease type 1A (CMT1A) (Lupski et al. 1991), suggesting that the two disorders may be the reciprocal products of unequal crossover during meiosis (Chance and Fischbeck 1994). Thus, *PMP22* acts in a dose-dependent manner, with a 50 % increased gene dosage leading to CMT1A and a 50 % reduction found in HNPP (Suter and Snipes 1995b). In addition to deletions, point mutations of *PMP22* have been recognized in HNPP, leading to a premature stop codon and causing a loss-of-function (Nicholson et al. 1994), as have other rare distinct mutations in the *PMP22* gene, resulting in altered expression of the PMP22 protein (Figure 1) (Stögbauer et al. 2000).

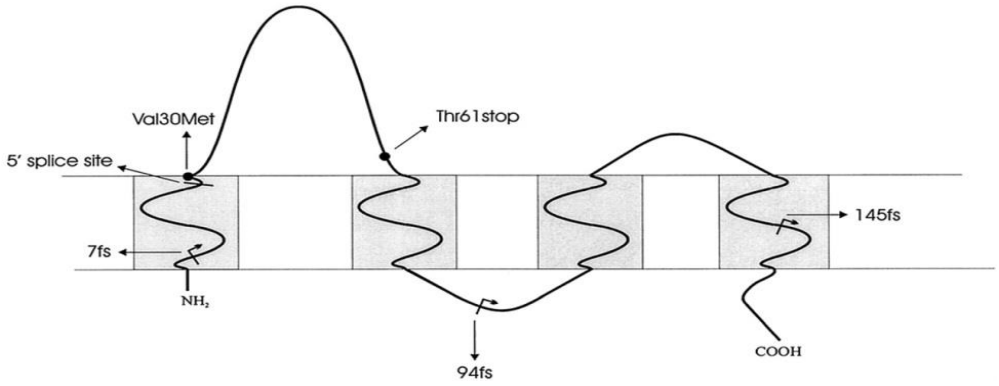

Figure 1: Schematic representation of the PMP22 mutations associated with HNPP. The PMP22 protein consists of two extracellular domains and four transmembrane domains. Three mutations (7fs, 145fs, Thr61stop) cause a functional loss of one PMP22 allele through premature termination of translation. A frameshift mutation (94fs) causes an elongated, probably nonfunctional PMP22 protein. The 5′-splice site mutation affects the normal splicing of PMP22 that leads to a mutant null allele. The de novo missense mutation (Val30Met) causes an amino acid substitution of the PMP22 protein (Stögbauer et al. 2000). Figure reproduced with kind permission of the author and the rights holder, Wolters Kluwer Health, Inc.

PMP22 is a 22 kDa hydrophobic, intrinsic membrane protein made up of 160 amino acids. Its precise biological functions are still unknown (Lupski et al. 1991; Jetten and Suter 2000; Li et al. 2013). This tetra-span protein is primarily expressed in myelinating Schwann cells (Chance et al. 1993; Jetten and Suter 2000), however, expression in non-nervous tissues, like the lung, the gut and the heart has been observed (Welcher et al. 1991; Quarles 1997). PMP22 comprises approximately 2-5 % of total myelin protein and is largely confined to compact myelin (Snipes et al. 1992; Pareek et al. 1993). *PMP22* upregulation has been shown to be induced during developmental myelination, as well as remyelination after peripheral nerve injury (Snipes et al. 1992). It has been suggested that the myelin protein serves as a structural component of myelin, responsible for adhesion between myelin membranes (Suter and Snipes 1995a), or has a role in controlling myelin sheath thickness and myelin integrity (Martini and Schachner 1997). Further observations have demonstrated that PMP22 and myelin protein zero (MPZ), the most abundant peripheral myelin protein (Ishaque et al. 1980) and a specific product of the Schwann cells (Brockes et al. 1980), may form complexes in the myelin membranes (D'Urso et al. 1999), probably participating in holding adjacent Schwann cells together, as well as in stabilizing myelin compaction (Martini et al. 2003). It has also been proposed that PMP22 is involved in proliferation, differentiation, and apoptosis of Schwann cells (Amici et al. 2007). More recently it has been found that PMP22 also plays a role in the linkage of the actin

cytoskeleton with the plasma membrane, possibly by regulating the cholesterol content of lipid rafts (Lee et al. 2014).

1.4. Histological hallmarks of HNPP

HNPP nerves form focal excessive myelin folds (tomacula) (Figure 2A) by unknown mechanism in sensory as well as in motor neurons (Oda et al. 1990). Tomacula are characterized by an extremely thickened myelin sheath wrapping around an axon of reduced diameter. Whether the reduced diameter is caused by a constriction of the axon by the thickened myelin or due to ongoing axonal atrophy is not fully clarified (Stögbauer et al. 2000). The sausage shaped swellings of the myelin sheath were first described by Behse et al. in 1972 (Behse et al. 1972a) and the name tomaculous neuropathy was proposed by Madrid and Bradley (Madrid and Bradley 1975), although focal myelin thickening can also be found in several other types of hereditary CMT diseases (Nordborg et al. 1984; Thomas et al. 1994) and even in IgM paraproteinemic neuropathy (Vital et al. 1985). Segmental demyelination (Figure 2B) and remyelination is found in sural nerve biopsies of HNPP patients (Behse et al. 1972b) and teased fiber preparations from these biopsies show a high frequency of tomacula, with over half of the fibers (54 %) affected (Sander et al. 2000). Madrid and Bradley described several mechanisms that may lead to the formation of a tomaculum, such as hypermyelination with redundant wrappings of the myelin sheath, excessive loop formation, two Schwann cells forming one myelin sheath and disruption of the myelin sheath (Madrid and Bradley 1975). Such abnormal myelin formations may arise from invaginations of myelin leading to myelin islands in mutant nerves, as observed in *Pmp22*$^{+/-}$ mice (Figure 3C) (Adlkofer et al. 1997). Studies with these transgenic mice have led to the hypothesis that tomacula are unstable structures that predispose to demyelination and that PMP22 is required for the flawless development of peripheral nerves, axon maintenance, myelin formation and the determination of myelin thickness and stability (Adlkofer et al. 1995).

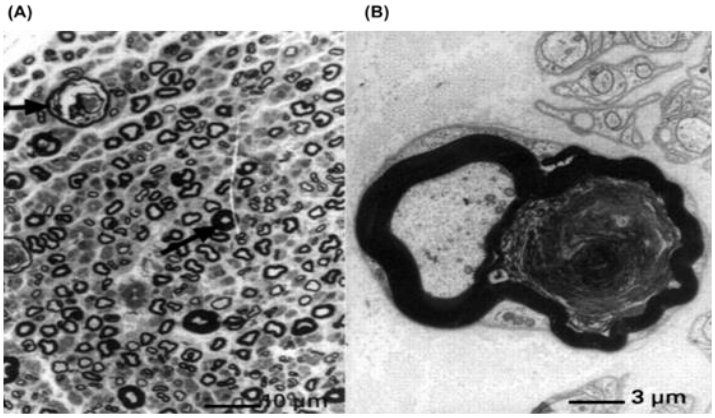

Figure 2: Histological features in HNPP. (A): Sural nerve from a patient with HNPP (transverse section). Top arrow: adaxonal myelin breakdown products; bottom arrow: hypermyelinated fibre. (B): Electron micrograph: a tomaculum with active myelin breakdown (modified from Sander et al. 2000). Figure reproduced with kind permission of the rights holder, BMJ Publishing Group Ltd.

Onion bulbs, excessive Schwann cell membrane processes around thinly myelinated axons (Li et al. 2013), are occasionally observed in HNPP nerves (Schenone 2006). These formations, more frequently observed in CMT1A, are seen as a sign of repeated cycles of de- and remyelination (Adlkofer et al. 1997; van Paassen et al. 2014).

1.5. Diagnostics

A typical clinical manifestation of HNPP is acute, painless, recurrent peripheral nerve palsies (Van Paassen et al. 2014). Electrophysiological examination is of great importance for the diagnostic progress, given the poverty of clinical findings (Dubourg et al. 2000). DNA testing for the *PMP22* gene deletion can confirm the diagnosis and sequencing of the *PMP22* gene can be used if no deletion is found. Nerve biopsies are not a standard method in establishing the diagnosis of HNPP (Van Paassen et al. 2014). Dubourg et al. have proposed guidelines for the diagnosis of HNPP patients, dividing the diagnostic criteria in 4 groups; clinical criteria (family history, age at onset, clinical manifestations, location of nerve palsies, clinical examination, course and severity and atypical presenting features), electrophysiological criteria, neuropathological features and molecular genetics (Dubourg et al. 2000).

1.6. Treatment

Treatment of HNPP is currently symptomatic. Transient bracing may be useful during a pressure palsy, and in the case of residual symptoms, permanent bracing may be needed (Bird 2014). Patients should be informed about avoiding activities that are risk factors for pressure palsies, such as prolonged sitting with legs crossed, repetitive movements of the wrist, prolonged leaning on elbows and rapid weight loss (Cruz-Martinez et al. 2000; Marriott et al. 2002). Excessive alcohol should be avoided and attention to careful positioning should be paid during operations (Rossor et al. 2015). Clinical improvement can be achieved through surgical decompression in the case of symptomatic carpal tunnel syndrome (Earle and Zochodne 2013). Vincristine used in chemotherapy has been reported to exacerbate HNPP (Kalfakis et al. 2002) through neurotoxicity (Zhu et al. 2013). Ethoxyquin, a synthetic antioxidant (Zhu et al. 2013) has in in vitro and in vivo studies shown to offer protection against the toxicity without impacting the effect of the chemotherapy (Chittoor-Vinod et al. 2015).

1.7. Transgenic mouse model for HNPP

Transgenic animal models serve as a tool for the elucidation of the underlying pathomechanisms of several disorders and provide a basis for the development of new therapeutic interventions and possible treatments. The genomic structure of the mouse *Pmp22* gene, situated in chromosome 11 (Suter et al. 1992), has been found to be identical to the human *PMP22* gene (Suter et al. 1994), which makes it a valuable model to work with for the understanding of the disease mechanism and to evaluate treatment strategies in peripheral neuropathies. *Pmp22*-deficient mice have been generated using gene targeting in embryonic stem cells (Adlkofer et al. 1995). These heterozygous *Pmp22* knock-out mice display similar morphological and electrophysiological features as observed in HNPP nerves; tomacula, electrophysiological abnormalities, as well as thinly myelinated axons and supernumerary Schwann cells forming onion bulbs (Adlkofer et al. 1997). Young $Pmp22^{+/-}$ mice have no electrophysiological abnormalities and lack clinical signs of a developing neuropathy. At the age of 12-14 months the mice show reduced amplitudes of the motor response (M-response) in the sciatic nerve, however, the NCVs are not significantly altered. $Pmp22^{+/-}$ mice are phenotypically indistinguishable from wild type mice, apart from sporadic walking difficulties observed in some individuals. Tomacula are rare in peripheral

nerve biopsies at postnatal day 24 but show an increased frequency at the age of 10 weeks (Adlkofer et al. 1995). The presence of many thick tomacula is a prominent feature in 10-month old mutant mice (Figure 3B). These tomacula, observed as sausage-like structures caused by focal hypermyelination, show a preferential paranodal location in teased nerve fiber preparations. They are unstable and degenerate progressively, culminating in a pathologic picture comparable to a demyelinating neuropathy (Suter and Nave 1999). Noncon-centrically arranged hypermyelinated structures around compressed axons (Figure 3E), as well as splitting of the dense line and vacuolation of myelin leading to myelin edema (Figure 3F) may be seen as early signs of myelin degeneration. The latter characteristic changes are in line with findings in biopsies from HNPP patients (Madrid and Bradley 1975; Adlkofer et al. 1997). At the age of 15 months, tomacula are still a prominent feature, but significant demyelination and onion bulb formation is also observed (Figure 3G-H) (Adlkofer et al. 1995).

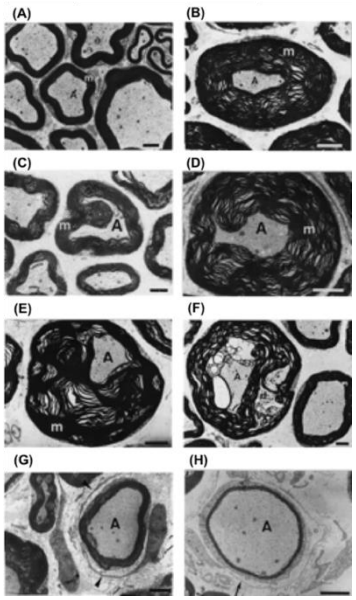

Figure 3: Cross sections of quadriceps nerves demonstrating abnormal myelin in *Pmp22*$^{+/-}$ mice. Pictures obtained by electron microscopy. (A): wild type mouse. (B): a 10-month old *Pmp22*$^{+/-}$ mouse showing hypermyelination by excessive wrapping of the myelin sheath. (C): a 10-month old *Pmp22*$^{+/-}$ mouse illustrating invagination of the myelin as a potential start of hypermyelination. (D): a 5-month old *Pmp22*$^{+/-}$ mouse showing intermyelin infolds forming a hypermyelin structure. (E): a 10-month old *Pmp22*$^{+/-}$ mouse showing a hypermyelin structure with a displaced axon. (F): a 10-month old *Pmp22*$^{+/-}$ mouse showing degenerating hypermyelin. (G and H): a 15-month old *Pmp22*$^{+/-}$ mouse showing onion bulbs (thinly myelinated axons with concentric Schwann cell processes (G, arrowheads) and basal laminae (H, arrow)). Markings: axons (A), compact myelin (m) and degenerating myelin (d). Scale bar: 2.5 µm (modified from Adlkofer et al. 1997). Figure reproduced with kind permission of the author and the rights holder, Society for Neuroscience.

It is hypothesized that focal sensory loss and muscle weakness in patients with HNPP are caused by reversible conduction block (CB) (Li et al. 2004) and explained by structural abnormalities at the nodes of Ranvier that lead to changes in axonal excitability. These abnormalities would predispose the nerves to CB when subjected to mechanical stress, such as pressure or stretch (Jankelowitz and Burke 2013). Further theories for the development of CB are discussed below. Experiments with mice demonstrate that mechanically induced CB occurs more rapidly and lasts longer in *Pmp22*$^{+/-}$ nerves than in wild type nerves. These findings are well in line with the focal symptoms, triggered by mild mechanical stress, in HNPP patients (Li et al. 2002; Bai et al. 2010). Focal constrictions in the axonal segments enclosed by, and decompacted myelin within the tomacula, have been observed in *Pmp22*$^{+/-}$ nerves. Reduced diameter in the constricted axons increases resistance to action potential propagation, thus predisposing these axons to CB. Furthermore, compression of the nerve may cause even further thinning of axons (Bai et al. 2010). Poor myelin compaction could impair the insulation of myelin, leading to excessive leakage of current. Essentially, decompacted myelin, along with constricted axons in the tomacula could predispose *Pmp22*$^{+/-}$ nerves to action potential propagation failure, enhanced by mechanical stress (Li et al. 2013). These findings suggest that a function of PMP22 is to protect the nerve from mechanical injury (Bai et al. 2010). Another possible explanation for CB lies in axonal hyperpolarization, found in both motor and sensory axons in HNPP patients. It has been hypothesized that the hyperpolarized resting membrane potential may cause changes in the nerve structure and could account for the development of CB after mechanical stress (Farrar et al. 2014). An alternative explanation for the impaired action potential propagation and nerve vulnerability to injury in HNPP is offered by impaired myelin junctions. The increase in myelin permeability and susceptibility to CB in *Pmp22*$^{+/-}$ nerves has been observed to take place prior to the formation of tomacula and demyelination. Furthermore, PMP22 deficiency has been shown to disrupt myelin junctions, such as tight junctions, leading to increased myelin permeability. This increased permeability impairs the electrical seal of myelin and is functionally comparable to demyelination (Guo et al. 2014). Yet another theory for the development of CB is offered in a study proposing a molecular pathway for the disrupted myelin junctions, in which myelin junctions were shown to be broken in regions with elevated p21-activated kinase (PAK1) activity. The enhanced activity of PAK1, a regulator of actin polymerization, correlated with increased levels of F-actin. Inhibition of PAK1 through pharmacological means normalized the levels of F-actin and arrested the progression of the myelin junction disruption and nerve CB (Hu et al. 2016).

1.8. Progesterone

Steroids are synthesized through a cascade of steps, the first being the conversion of cholesterol to pregnenolone, the precursor of all steroid hormones. A limiting step in the pregnenolone formation is the transport of cholesterol from intracellular stores to the inner mitochondrial membrane, where the cholesterol side-chain-cleaving cytochrome P450scc is located (Schumacher et al. 2012). Progesterone present in the nervous system derives from the circulation, but can also be synthesized from pregnenolone by neurons and glial cells. Steroids synthesized in the nervous system have been named neurosteroids (Baulieu 1997), and several studies in experimental models of peripheral neuropathies indicate that they act as protective agents in the CNS as well as the PNS (Giatti et al. 2015).

Schwann cells synthesize progesterone in the peripheral nervous system (Koenig et al. 1995), where it plays an important role in the formation of myelin sheats (Koenig et al. 1995; Schumacher et al. 2001). The promoting effect of progesterone on myelin formation has been shown in vitro in co-cultures of Schwann cells and sensory neurons (Chan et al. 1998), in explant cultures of rat dorsal root ganglia, and in vivo, after cryolesion of the mouse sciatic nerve (Koenig et al. 1995). Progesterone increases promoter activity of *PMP22*, acting on promoter 1, but not on promoter 2 of the corresponding gene (Désarnaud et al. 1998). Transcripts originating from promoter 1 mainly reside in the PNS and are associated with myelin formation during development and regeneration, whereas transcripts from promoter 2 are abundant in non-neuronal tissue and less correlated with myelin formation (Bosse et al. 1994; Suter et al. 1994). Furthermore, progesterone and its derivates have been shown to induce *PMP22* expression in vitro, as well as in vivo (Melcangi et al. 1999; Notterpek et al. 1999; Sereda et al. 2003).

Progesterone stimulates expression of myelin proteins through interaction with the classical progesterone receptor (PR) (Meyer zu Hörste et al. 2006; Sereda and Nave 2006) (Figure 4). Not only do Schwann cells synthesize progesterone, they also express the intracellular receptor for the neurosteroid, indicating its participation in autocrine signaling in the PNS (Jung-Testas et al. 1996). The PR, a ligand-induced transcription factor, has been shown to be important in the activation of myelin genes (Meyer zu Hörste et al. 2006; Sereda and Nave 2006). Binding of progesterone to the progesterone receptor monomer in the cytosol leads to the dimerization of the monomer and a translocation to the nucleus

(Beato 1989; McKenna and O'Malley 2002). The progesterone-progesterone receptor complex binds to specific DNA sequences, called progesterone response elements (PRE), and regulates the gene expression together with co-activators and co-repressors (McKenna and O'Malley 2002; Wu et al. 2005). An alternative to this classical view of activation is offered by evidence that suggest that PR monomers may be even more efficient transactivators of the responsive DNA elements than PR dimers (Jacobsen et al. 2009; Jacobsen and Horwitz 2012).

The effects of progesterone on myelin protein genes seem to be indirect, as their promoter regions do not contain classical progesterone response elements. Instead, progesterone may induce myelination by increasing the expression of transcription factors involved in Schwann cell differentiation and myelination (Guennoun et al. 2001). In fact, progesterone has been shown to stimulate the expression of Early Growth Response 2 (*EGR2/KROX-20*, hereafter referred as *KROX-20*) (Guennoun et al. 2001; Mercier et al. 2001), a transcription factor required for *PMP22* activation, by binding to its intracellular receptor in Schwann cells. Indeed, the promoter sequence of *KROX-20* contains regions of high homology for the PRE (Guennoun et al. 2001).

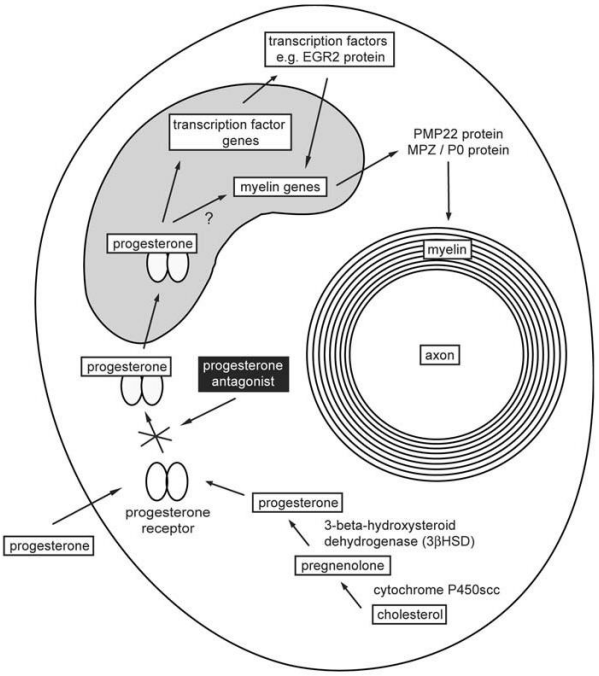

Figure 4: The effect of progesterone on PMP22. Schwann cells synthesize progesterone from cholesterol. Endogenous and exogenous progesterone bind to the progesterone receptor (PR) and the PR monomers dimerize. The progesterone-PR-complex translocates to the nucleus of the Schwann cells where it activates the transcription factor EGR2/KROX-20, leading to an upregulation of the myelin protein gene PMP22 (Meyer zu Hörste et al. 2006). Figure reproduced with kind permission of the author and the rights holder, Springer Nature.

1.9. KROX-20

KROX-20 is a zinc finger transcription factor expressed in Schwann cells and a key regulator of myelin genes during early development (Topilko et al. 1994; Le et al. 2005; Decker et al. 2006). It is activated in Schwann cells after axonal contact, before myelination (Topilko et al. 1994; Murphy et al. 1996), and expressed throughout myelination and during adult life (Zorick et al. 1996). KROX-20 is required for induction of *PMP22* expression (Nagarajan et al. 2001; Le et al. 2005). Progesterone stimulates the expression of *KROX-20* as well as other transcription factors with a key role in Schwann cell physiology and myelination (Guennoun et al. 2001; Mercier et al. 2001; Magnaghi et al. 2007). Loss of KROX-20 has been shown to lead to myelin breakdown, and inactivation of the transcription factor in adult Schwann cells results in demyelination involving Schwann cell dedifferentiation, indicating a role of KROX-20 in maintaining the myelin sheath. Following injury, the axon and its myelin sheath distal to the lesion degenerate in a process known as Wallerian degeneration (Fawcett and Keynes 1990) and loss of *KROX-20* ex-

pression is likely to constitute a key step in this process (Stoll and Müller 1999). Overexpression of *KROX-20* induces the expression of *PMP22* in Schwann cell cultures (Nagarajan et al. 2001) and no expression of myelin proteins takes place in Schwann cells of *Krox-20* $^{-/-}$ mice (Topilko et al. 1994). Studies on these *Krox-20* knock-out mice show that the differentiation of myelinating Schwann cells arrests at the promyelinating stage, the major myelin proteins are not expressed and myelin is not formed (Topilko et al. 1994; Zorick et al. 1999).

1.10. Aims of the study

Very few publications concerning the HNPP mouse model have been published and hence there is little awareness of its features and phenotypic resemblance to human patients. The first aim of this thesis is to study the model on a genetic, histological and electrophysiological level and to review existing published data and to compare it to the results obtained. This data is subsequently used to perform a comparison between the phenotype of the rodent model to the known features in HNPP patients, and to make an estimation of the suitability of the mouse model as a reliable tool for HNPP studies.

The second aim is to examine the short- and long-term effects of progesterone in the mouse model for HNPP. Progesterone has been shown to induce *PMP22* expression both in vivo and in vitro. Since HNPP is caused by a decreased amount of PMP22, increasing the gene dosage may be a therapeutic target, and progesterone a potential substance to achieve this. Progesterone exerts its effect on *PMP22* expression through activation of the transcription factor KROX-20, a necessary step for the initiation of myelin formation in peripheral nerves. In this study, the emphasis is laid on observing the therapeutic effects on a molecular, histological and electrophysiological level; by measuring the levels of *Pmp22* and *Krox-20* mRNA, by quantifying histological features of the peripheral nerve, and by performing electrophysiological measurements. To date, no published data exists on the effects of a progesterone therapy on *Pmp22* $^{+/-}$ mice. Moreover, only symptomatic treatment is currently available for patients with HNPP.

2. Materials and methods

2.1. Materials

2.1.1. Consumables

CO_2	Messer-Griesheim, Krefeld
Coverplates	Menzel-Gläser, Braunschweig
Disposable gloves (latex, nitril)	Hartmann, Heidenheim
Dry ice	Messer-Griesheim, Krefeld
Eppendorf cups: 0.5 ml, 1.5 ml, 2 ml	Eppendorf, Hamburg
Falcon tubes: 15 ml, 50 ml	Beckton & Dickinson, Le Pont De Claix, France
Liquid nitrogen	Messer-Griesheim, Krefeld
Object slides	Menzel-Gläser, Braunschweig
Parafilm "M"	American National Can™, Chicago
PCR microtiter plates	ABgene, Surrey, UK
PCR plate foils "Air Pore Sheet"	ABgene, Surrey, UK
Pipette tips	Molecular Bioproducts, San Diego, CA, USA
Sutures	Fine Science Tools, Heidelberg
Syringes	Beckton & Dickinson, Le Pont De Claix, France
Tissues	Wepa professional, Arnsberg

2.1.2. Chemicals and reagents

Acetic acid	Merck, Darmstadt
Agarose	AppliChem, Darmstadt
Ammonium acetate	Merck, Darmstadt
Azure II	Merck, Darmstadt
Beta-Mercaptoethanol	Merck, Darmstadt
Chloroform	Merck, Darmstadt
DDSA (2-Duodecenyl-succinicacidanhydrid)	Serva, Heidelberg

di-Sodium hydrogen phosphate dihydrate ($Na_2HPO_4 *2H_2O$)	Merck, Darmstadt
DMP30 (2,4,6-Tris-dimethylaminomethyl-phenol)	Serva, Heidelberg
DTT (1,4-Dithiotreitol)	GibcoBRL, Karlsruhe
EDTA (Ethylenediaminetetraacetic acid)	Merck, Darmstadt
Ethanol	Merck, Darmstadt
Ethidium bromide	Sigma-Aldrich, Schnelldorf
Eukitt® quick-hardening mounting medium	Kindler, Freiburg
Glutardialdehyde	Merck, Darmstadt
Hydrogen chloride (HCl)	Serva, Heidelberg
Isopropanol	Merck, Darmstadt
Methanol	Merck, Darmstadt
Methyl nadic anhydride (MNA)	Serva, Heidelberg
Methylene blue	Merck, Darmstadt
Osmium tetroxide	Serva, Heidelberg
Paraformaldehyde	Serva, Heidelberg
Pellet Paint® Co-Precipitant	Merck, Darmstadt
Propylene glycol (1,2-Propanediol ReagentPlus®)	Sigma-Aldrich, Schnelldorf
Sodium chloride (NaCl)	Merck, Darmstadt
Sodium dihydrogen phosphate monohydrate ($NaH_2PO_4 *H_20$)	Merck, Darmstadt
Sodium hydroxide (NaOH)	Merck, Darmstadt
TRIS (Tris-(hydroxymethyl)-aminomethane)	Roth, Karlsruhe
Triton™ X-100	Sigma-Aldrich, Schnelldorf
Xylol	Merck, Darmstadt

2.1.3. Buffers and solutions

Epoxy resin embedding solution (Luft 1961)

Epoxy solution A:

Glycidyl ether	67.5 g

DDSA	88.2 g

→ Stir with a magnetic stirrer for 1 h

Epoxy solution B:

Glycidyl ether	82.3 g
MNA	73.3 g

→ Stir with a magnetic stirrer for 1 h

Epoxy embedding solution:

→ Mix Epoxy solution A and B and add 1.8 % DMP-30

Fixation solution (Karlsson and Schultz 1965)

Sodium dihydrogen phosphate *H_20	0.36 g
Disodium hydrogen phosphate *$2H_20$	3.1 g
NaCl	1 g
Glutardialdehyde solution	20 ml
Paraformaldehyde	8 g

→ Dissolve PFA in 60 ml ddH_2O by stirring at 60-70 ^oC. Add ddH_2O to a total volume of 80 ml. Add 1 M NaOH until the solution is clear. Filter the solution with a sterile filter and adjust the pH to 7.4. Dissolve the salts (NaH_2PO_4, Na_2HPO_4, NaCl) in 100 ml ddH_2O and add to the PFA-solution.

Methylene-Azure-II staining solution (Richardson et al. 1960)

Methylene blue solution:

→ Methylene blue in 1 % Borax solution

Azure-II solution:

→ 1 % Azure II in H_2O

Methylene-Azure-II staining solution:

→ Mix both solutions 1:1

TAE buffer (50x)

TRIS-HCl	242 g

Acetic acid 100 %	57.1 g
EDTA (0.5 M; pH 8)	100 ml
→ Add ddH_2O to a total volume of 1000 ml	

5X Green GoTaq® Reaction buffer (Promega, Mannheim)

2.1.4. Enzymes and reaction kits

GoTaq® DNA polymerase	Promega, Mannheim
Power Sybr® Green PCR Master Mix	Applied Biosystems, UK
Proteinase K	Boehringer, Mannheim
RNeasy Mini Kit	Qiagen, Hilden
RNA 6000 Nano Assay	Agilent Technologies, Böblingen
Superscript-III-RT Kit	Invitrogen, Carlsbad, CA, USA
TRIzol Reagent	GibcoBRL, Karlsruhe

2.1.5. Pharmaceuticals

Aureomycin® eye ointment	Riemser, Greiswald – Insel Riems
Ketamine (Ketanest®)	Parke-Davis, Berlin
Progesterone powder	Sigma-Aldrich, Schnelldorf
Time Release Pellets, 60 Day Release (Progesterone, Placebo)	Innovative Research of America, Sarasota, Florida, USA
Time Release Pellets, 90 Day Release (Progesterone, Placebo)	Innovative Research of America, Sarasota, Florida, USA
Xylazine (Rompun®)	Bayer, Leverkusen

2.1.6. Nucleic acids

Desoxyribonukleoside triphosphates (dNTPs)	Boehringer, Mannheim
GeneRuler 100 bp DNA Ladder	Thermo Fischer Scientific, Waltham, MA, USA
Random nonamer primers	Max-Planck-Institute for Experimental Medicine, Göttingen

2.1.7. Oligonucleotides

The primer oligonucleotides were synthesized in the sequencing department of Max-Planck-Institute for Experimental Medicine (Göttingen).

Primers for genotyping *Pmp22*$^{+/-}$ mice:

Pmp22 transgene *Forward*: 5'-GCATCGAGCGAGCACGTAC-3´

Pmp22 transgene *Reverse*: 5'-ACGGGTAGCCAACGCTATGTC-3'

Primers for genotyping wild type mice:

Pmp22 wild type *Forward*: 5'-CAGCCACCATGCTCCTACTC-3'

Pmp22 wild type *Reverse*: 5'-CAGCCCTTGCTCACTGTCTAC-3'

Primers for real-time PCR with Sybr®-Green:

β-actin *Forward*: 5'-CGCTCAGGAGGAGCAATG -3'

β-actin *Reverse*: 5'-TGACAGGATGCAGAAGGAGA -3'

Cyclophilin *Forward*: 5'-CACAAACGGTTCCCAGTTTT-3'

Cyclophilin *Reverse*: 5'-TTCCCAAAGACCACATGCTT-3'

Pmp22 *Forward*: 5'-AATGGACACACGACTGATC-3'

Pmp22 *Reverse*: 5'-CCTTTGGTGAGAGTGAAGAG-3'

Rplp0 *Forward*: 5'-GATGCCCAGGGAAGACAG-3'

Rplp0 *Reverse*: 5'-ACAATGAAGCATTTTGGATAATCA-3'

Rps20 *Forward*: 5'-GAACAAGTCGGTCAGGAAGC-3'

Rps20 *Reverse*: 5'-ATTCGGTGAATCGCCACTT-3'

Krox-20 *Forward*: 5'-GCAGAGATGGGAGCGAAGC-3'

Krox-20 *Reverse*: 5'-AGATGAACGGAGTGGCGG-3'

2.1.8. Equipment and instrumentation

Agarose gel chamber and combs	Technical department, Max-Planck-Institute for Experimental Medicine, Göttingen
Agarose gel documentation "ImageMaster VDS"	Amersham Pharmacia Biotech, Freiburg
Agilent Bioanalyzer	Agilent Technologies, Böblingen
Axiophot light microscope	Zeiss, Oberkochen
Centrifuge 4K15C	Sigma, Osterode am Harz
Centrifuge 5403	Eppendorf, Hamburg
Combi Thermosealer PCR plate sealer	Advanced Biotechnologies, Surrey, UK
Diamond knife	Diatome AG, Biel, Switzerland
Digital camera for light microscope	Kappa obstronics GmbH, Gleichen
Dissection kit	Fine Science Tools, Heidelberg
Electronic 8-channel pipette	Eppendorf, Hamburg
Fridge (+4 °C)	Liebherr, Ochsenhausen
Freezer (-20 °C)	Liebherr, Ochsenhausen
Freezer (-85 °C) Ultra Low Freezer	New Brunswick Scentific, Nürtingen
Jaeger-Toennis Neuroscreen	Jaeger-Toennies, Würzburg
Gel electrophoresis power supply	Amersham Pharmacia Biotech, Freiburg
Glassware	Schott, Mainz
Leica EM Trim Specimen Trimmer	Leica Microsystems, Wetzlar
Innova 4000 Incubator Shaker	New Brunswick Scientific, Nürtingen
LightCycler® 480 Real-Time PCR System	Roche Diagnostics, Mannheim
Lynx el tissue processor	Vision Biosystems Inc., Australia
Magnetic stirrer RCT basic Ikamag	Omnilab, Bremen
Microwave oven	AEG, Frankfurt a.M.
Multipipette® plus	Eppendorf, Hamburg

PCR Thermocycler T3	Biometra, Göttingen
Pipettes (2, 10, 100, 200, 1000 µl)	Gilson, Middelton, WI, USA
Precision weighing balance (digital)	Sartorius, Göttingen
Ultracut S microtome	Leica, Wetzlar
Ultrapure water system Arium 611 VF	Sartorius, Göttingen
Ultraturrax T8 tissue homogenisator	IKA Labortechnik, Staufen
Vortex-Genie-2 vortex mixer	Bender & Hobein GmbH, München
Water bath	Gesellschaft für Labortechnik, Burgwedel

2.1.9. Software

Adobe Photoshop CS5	Adobe Systems Software, Saggart, Ireland
Excel 2003	Microsoft Europe, Berlin
geNorm 3.5	Center for Medical Genetics, Ghent, Belgium (Vandesompele et al. 2002)
GraphPad Prism® 5.0	GraphPad Software, La Jolla, CA, USA
Image J. 1.40g	NIH, USA
PyRAT	Scionics Computer Innovation, Dresden
qBase 1.3.5	Center for Medical Genetics, Ghent, Belgium
Statistica 6.0	StatSoft Europe, Hamburg
Word 2003	Microsoft Europe, Berlin

2.2. Methods

2.2.1. Animal breeding and maintenance

2.2.1.1. HNPP mouse model

An ethical permission for the study was obtained from "Niedersächsisches Landesamt für Verbraucherschutz und Lebensmittelsicherheit" (LAVES) (file number: 33.9-42502-04-10/0285). The mice were bred and maintained in the animal facilities of the Max Planck Institute for Experimental Medicine (Göttingen) in accordance with the recommendations of the German Society for Laboratory Animal Science (GV-SOLAS). Before and throughout the study the animals obtained free access to food and water.

Mice used in the experiments originated from the breeding strain Agouti SV129 EV/C57BL/6 (Adlkofer et al. 1995), acquired through breeding of wild type females (*Pmp22*$^{+/+}$) with heterozygous *Pmp22*$^{+/-}$ males. The offspring were therefore wild type or expressed a *Pmp22*$^{+/-}$ genotype. The wild types served as controls in the subsequent studies, while the heterozygote *Pmp22*$^{+/-}$ mice (hereafter referred as HNPP mice) were used either as treatment animals or placebo-controls. Male mice were exclusively used in the studies in order to avoid the cyclic fluctuating levels of progesterone in female mice.

2.2.1.2. Identification of the study animals

The mice were identified through ear markings, consisting of numbers from 1-99 (Figure 5). These were given under light anesthesia at the age of three weeks. Identification cards marked the cages where the mice where kept. These contained information about the identification number, the date of birth, the gender, the breeding strain, the litter number, and the identification number of the parents. Skin biopsies from the tip of the tail were obtained at the same time as the ear markings were given. These were stored at -20 ^{o}C and subsequently used for genotyping with PCR. The mice and the cages were administered with the PyRAT Software (Scionics Computer Innovation).

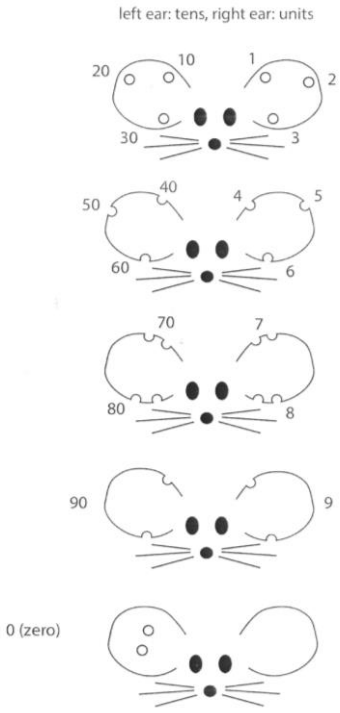

Figure 5: Ear markings. The mice were identified through ear markings. The marks on the left ear (when seen from the front) represent numbers from 1-9, the marks on the right ear represent numbers from 10-90.

2.2.2. Study design and groups

2.2.2.1. Experimental dosage-finding pilot study with progesterone on HNPP mice

A short-term pilot study, testing two different dosages of progesterone, was performed on HNPP mice before the commencement of the long-term therapy studies. *Pmp22* mRNA expression served as a surrogate parameter for treatment effectiveness. Injections of the steroid were applied subcutaneously in two different dosages (10 mg/kg bw and 40 mg/kg bw). Progesterone was dissolved in propylene glycol, and applied in a volume of 100 µl every second day for nine days, the daily dosage hence being 5 or 20 mg/kg bw. The HNPP controls were similarly given a placebo, i.e. the same amount of propylene glycol. The first injections were given to adult mice aged 13 to 16 weeks. The mice were sacrificed eight hours after the last injection through cervical dislocation, and the sciatic nerves (*N. ischiadici*) were resected and stored at -85 ^{o}C for subsequent RNA precipitation. The treatment groups were as follows:

Treatment:	Number of animals:
Progesterone 10 mg/kg bw	5
Progesterone 40 mg/kg bw	4
Placebo	7
No treatment (wild type mice)	4

2.2.2.2. Long-term therapy studies

The long-term experiments were performed on male HNPP mice and wild type mice. The animals were genotyped at the age of three weeks and divided in a randomized manner into three groups. The heterozygote carriers of the *Pmp22* gene were either treated with progesterone (HNPP treatment group) or with a placebo substance (HNPP control group). The third group consisted of wild type mice, which obtained neither progesterone, nor placebo (wild type control group).

Two long-term therapy studies were carried out. In one the animals were treated for 60 days with a subcutaneous progesterone or placebo pellet (Figure 6A). In the other study the animals obtained two subsequent pellets containing the same substance for a total of 150 days (Figure 6B). The first implanted pellet contained 50 mg progesterone or placebo and had a release time of 60 days. The second pellet had a concentration of 75 mg of progesterone or placebo and a release time of 90 days. The pellets followed zero order kinetics, releasing a constant, even amount of the active product for the designed release time.

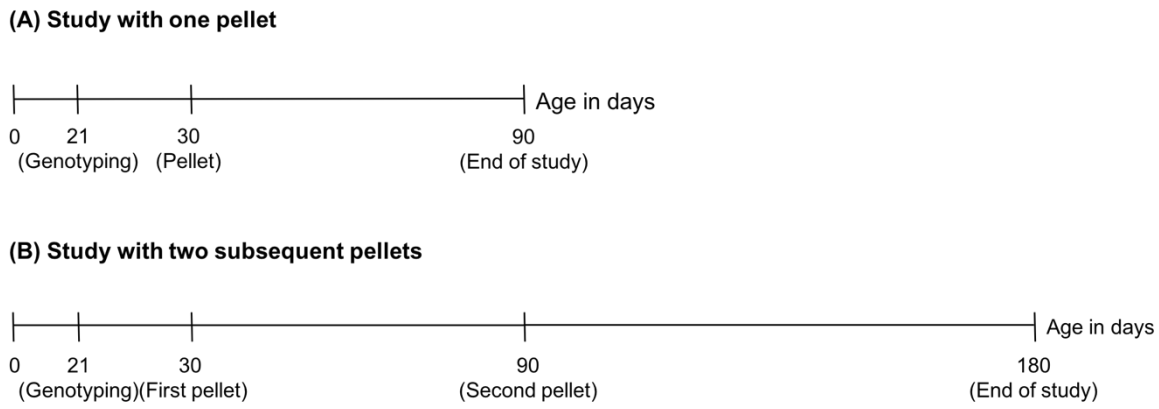

Figure 6: Timeline describing the phases of the two long-term studies. The mice were born at P0 and the first pellet was implanted at P30. (A): The treatment period for the first study was 60 days (2-month study) and ended at P90. (B): The mice from the second study received their second pellet at P90 and the total treatment period of the two subsequent pellets was 150 days (5-month study). The study ended at P180.

2.2.2.3. Subcutaneous implantations of progesterone and placebo pellets

The first pellets were implanted at the age of 30 days and the second ones at the age of 90 days. A 1 cm incision was made on the back of the neck, 1 cm posterior to the ear, and the pellet was inserted in a skin pocket, formed by using a blunt, sterile instrument. The wound was closed with sutures.

2.2.2.4. Anesthesia of the study animals

The subcutaneous implantations of the pellets, as well as the electrophysiological analysis, followed under full anesthesia with intraperitoneal injections of 5 mg/kg bw ketamine (Ketanest®) and 2 mg/kg bw xylazine (Rompun®). Aueromycin® eye ointment was applied to the eyes of the mice during narcosis in order to prevent drying of the open eyes.

2.2.2.5. Preparation of peripheral nerves

The mice were sacrificed through cervical dislocation at the end of the studies, and the *N. ischiadici* were resected. One of the nerves was immediately frozen down and stored at -85 ^{o}C for subsequent RNA precipitation, and the other one was stored at 4 ^{o}C posterior to fixation with phosphate-buffered glutaraldehyde (Karlsson and Schultz, 1965).

2.2.3. Molecular biology methods

2.2.3.1. Genotyping the study animals

2.2.3.1.1. DNA extraction

Genomic DNA was extracted from the tail biopsies using a lysis solution (22.92 µl 10x MGB, 11.46 µl 10 % Triton X-100, 916.72 µl proteinase K and 194.8 µl distilled water) and incubating at 55 ^{o}C over night. The extracted DNA was stored at 4 ^{o}C and diluted in 900 µl water prior to the use in the polymerase chain reaction.

2.2.3.1.2. Polymerase chain reaction (PCR) of genomic DNA

The genotyping of the mice was performed with polymerase chain reaction, a standardized method for amplifying a specific sequence of DNA in vitro. This method, widely used in molecular biology and medicine, dates back to 1986 (Mullis et al. 1986). The principle

relies on repeated cycles of heating and cooling of the reaction; denaturation of the complementary strands at 94 ºC, annealing of the sequence-specific oligonucleotides (primers) at 61 ºC and elongation of the new DNA strands at 72 ºC. A heat-stable DNA polymerase (Taq polymerase), originally isolated from the bacterium *Thermus aquaticus*, enables the exponential amplification of the DNA template.

The specific sequence for the *Pmp22* transgene was amplified in order to distinguish the HNPP mice (*Pmp22*$^{+/-}$) from the wild types (*Pmp22*$^{+/+}$). The PCR was carried out with the GoTaq® polymerase (Promega), using the following reaction mix and amplification protocol:

DNA	0.5 µl
5X Green GoTaq® Reaction buffer	4 µl
dNTPs (2.5 mM each)	1 µl
3´-Primer	0.1 µl
5´-Primer	0.1 µl
GoTaq® DNA Polymerase (1.6 U/50 µl)	0.1 µl
Aq. dest.	14.2 µl

1 min - 94 ºC
35 cycles: 1 min - 61 ºC; 1 min - 72 ºC; 1 min - 94 ºC
1 min - 61 ºC
5 min - 72 ºC

2.2.3.1.3. Agarose gel electrophoresis of the PCR products

Agarose gel electrophoresis is a method for separating DNA fragments according to their length. DNA, being negatively charged, moves in an electric field through the agarose matrix in the direction of the positive pole, shorter fragments separating faster than longer ones due to the better pore size/mass ratio. The separated fragments can be visualized with ethidium bromide under UV-light.

A 1-1.5 % gel was made by dissolving agarose powder in heated 1x TAE buffer. Ethidium bromide (1µl/ml) was added, the gel was poured into a cast, and a comb was placed in the chamber to create wells for the samples. 1x TAE buffer was used as running buffer and the

probes were run at 90-150 V. The separated fragments were visualized under UV-light, using the ability of ethidium bromide to intercalate in DNA. The length of the fragments was determined using Generuler 100 bp (Thermo Fischer Scientific) as ladder. The HNPP mice presented two bands of the size of 260 bp and 317 bp, whereas the wild type littermates only showed one 317 bp band.

2.2.3.2. cDNA transcription and amplification from isolated RNA

2.2.3.2.1. RNA isolation

RNA was isolated from the resected *N. ischiadici* with Qiagens´s "RNeasy Mini Kit", using the protocol for small fatty tissues. The frozen samples were transferred into 1 ml TRIzol reagent and homogenized with a tissue homogenizator for 30 s (Ultraturrax T8). TRIzol works by maintaining RNA integrity during homogenization, while at the same time disrupting and breaking down cells and cell components. The samples were incubated at room temperature for 5 min to permit complete dissociation of the nucleoprotein complex, and 200 µl of chloroform was added. The samples were mixed vigorously, incubated at room temperature for 3 min and centrifuged for 15 min at 14000 rpm at 4 ^{o}C. The upper aquatic phase containing RNA was transferred into a new eppendorf cup. The equal volume unit of 70 % ethanol (EtOH) was added. 700 µl of this mixture was moved to an RNeasy Mini Spin Column. The columns were loaded and washed with 700 µl RW 1 buffer and twice with 500 µl RPE buffer. The remaining EtOH was removed through centrifugation for 3 min at 14000 rpm. The columns were transferred to eppendorf cups and the RNA was eluted from the silicate membrane. This was done by pipetting 50 µl of RNase-free water directly on the membrane, centrifuging 1 min at 12000 rpm and repeating this step with the flow-through.

2.2.3.2.2. Quantification and qualification of RNA

RNA quantity, quality (degree of contamination) and integrity (degradation) were measured with Agilent Bioanalyzer, using the RNA 6000 Nano Assay. Small amounts of RNA (1 µl, ca. 50 pg) are sufficient for analysis with this assay, in which microfluidic capillary electrophoresis is used to separate total RNA in a sieving polymer matrix according to molecular weight. As RNA runs through the gel matrix, it binds to a fluorescence dye and gives a signal in the form of bands and an electropherogram. Since ribosomal RNA

(rRNA) represents over 90 % of the total RNA, the measurements reflect the quality of the rRNA. An uncontaminated sample yields two bands, representing the sedimentation coefficients for the rRNA: 18S and 28S. The concentration of the RNA sample is determined by comparing the intensity of its signal to that of a ladder with a known concentration.

A gel was prepared by centrifuging 400 µl RNA gel-matrix through a filter tube at 2500 rpm and mixing it with 130 µl RNA dye. 9 µl of this mixture was loaded and pressed into the capillaries of an RNA chip with a Chip Priming Station (Agilent Technologies). A Nano marker was pipetted in each well, and an RNA ladder was used as a reference for the quantities and sizes of the RNA samples. The quality of the samples was determined through the integrals of the fluorescence signals from the 18S- and 28S RNA, the optimum being 28S/18S = 2.1. A degradation of the RNA would have been seen as a dispersion of the two peaks, and an increase in the retention time would have reflected contamination of the samples.

2.2.3.2.3. RNA precipitation

The concentration of the RNA was increased through precipitation, a process in which salts are used to neutralize the charge of the nucleic acid backbone, causing RNA to become less hydrophilic and fall out of solution. 1.5 µl Pellet Paint®, a glycogen-based co-precipitant, was added to the samples and the samples were mixed, followed by addition of 0.5 volume units of 7.5 M ammonium acetate. The RNA was precipitated with 2.5 volume units of 100 % EtOH and separated through centrifugation for 2 min at 13000 rpm at 4 ºC. Due to the pink color given by the Pellet Paint®, the pellet was easily identified, and the supernatant could be removed. Remaining salts were removed through washing the pellet twice with 200 µl 70 % EtOH and removing the EtOH through suction. The pellet was dried for 30 min on ice and thereafter dissolved into 10 µl RNase-free water.

2.2.3.2.4. cDNA synthesis

The isolated RNA from the *N. ichiadici* was converted into complementary DNA (cDNA) through reverse transcription PCR (RT-PCR) with the "Superscript-III-RT" kit. This enabled its use as a probe for the subsequent expression analysis with real-time PCR. Oligo-dT primers (0.6 µM) were used to transcribe mRNA into cDNA, as they only prime at pol-

yadenylated mRNA, complementary to their poly-T tails. The efficiency of the synthesis was increased through the use of random Nonamer primers (N9 primer, 120 µM).

2 µl Oligo dT primer and 2 µl N9 primer was added to the RNA samples (250 ng), followed by an incubation for 1 min at 70 °C, during which the primers annealed to the mRNA. The reaction mix was cooled down on ice and a mixture of 4 µl 5x 1st strand buffer, 2 µl 1M dichlordiphenyltrichlorethan (DTT), 1 µl dNTPs (10mM) and 1 µl "Superscript III" polymerase (200 U/µl) was added. The cDNA synthesis was performed with incubation steps as follows:

10 min - 25 °C
45 min - 50 °C
45 min - 55 °C

2.2.3.2.5. Semiquantitative real-time polymerase chain reaction with Sybr®-Green

The cDNA was amplified with real-time PCR, a technique that follows the general principle of polymerase chain reaction and, in addition, detects and quantifies DNA as it is amplified. The amplified DNA was detected with Sybr®-Green, a cyanine dye (Morrison et al. 1998) that emits fluorescence as it binds to double-stranded DNA. The amount of fluorescence measured after each PCR cycle correlates to the amount of the DNA product. A disadvantage of Sybr®-Green is its ability to bind double-stranded DNA in an unspecific manner, including primer dimers and contamination with genomic DNA. This makes the design and use of well-designed primers specific to the cDNA utterly important. Primers flanking introns prevent the amplification of genomic DNA because the short extension time is not sufficient to perform this, however being long enough for the amplification of the short cDNA.

Quantification of the DNA relies on plotting the fluorescence against the number of cycles on a logarithmic scale. The threshold cycle (Ct) gives the number of cycles at which the fluorescence exceeds a given threshold, the value being lower the higher the concentration of the used target DNA is. The Ct value is normalized to the values of "housekeeping genes". These genes have relatively constant expression levels and serve as a measure for the amount of cDNA in each sample. The transcription rate of the examined gene is expressed proportionally to that of the housekeeping genes. The fact that the expression is

normalized to that of the housekeeping genes, gives the name “semiquantitative” to this type of real-time PCR.

The validity of the results was augmented by using several housekeeping genes and normalizing the expression rate to that of the mean of these standards. The most suitable combination of housekeeping genes with the smallest variation in expression rates between the different samples was identified with the “geNorm 3.5” software (Vandesompele et al. 2002 #114). The analysis of the Ct raw data was performed with the “q-Base 1.3.5” software (Hellemans et al. 2007). The following reaction mix was used:

cDNA	2 µl
Sybr®-Green Master mix	5 µl
5´-Primer (50 µM)	0.2 µl
3´-Primer (50 µM)	0.2 µl
Aq. dest.	2.6 µl

The semiquantitative real-time PCR was performed with LightCycler® 480 Real-Time PCR System according to the following amplification protocol:

2 min - 50 °C
10 min - 95 °C
40 cycles: 15 s - 95 °C; 60 s - 60 °C

2.2.4. Histological methods

2.2.4.1. Embeddings in epoxy resins

The resected *N. ischiadici* stored in gluteraldehyd were embedded in epoxy resins (epon), a class of reactive polymers. This enabled the preparation of semithin slices for light microsopy. First, the samples were fixated and stained with osmium tetroxide (O_5O_4) and dehydrated with a rising concentration of EtOH. The EtOH was washed away with propylene oxide in order to allow the infiltration of the samples in epoxy. These steps followed automatically with a “Lynx el” tissue processor, according to the following program:

Solution	Time	Temperature
Phosphate buffer (0.1 M)	15 min	4°C
2 % O_sO_4	4 h	4°C
Aq. dest.	20 min	RT
Aq. dest.	20 min	RT
Aq. dest.	20 min	RT
30 % EtOH	30 min	RT
50 % EtOH	30 min	RT
70 % EtOH	30 min	RT
90 % EtOH	30 min	RT
100 % EtOH	30 min	RT
100 % EtOH	15 min	RT
100 % EtOH	15 min	RT
100 % EtOH	15 min	RT
100 % EtOH	15 min	RT
Propylene oxide	15 min	RT
Propylene oxide	15 min	RT
Propylene oxide	15 min	RT
Propylene oxide/Epon 2:1	2 h	RT
Propylene oxide/Epon 1:1	2 h	RT
Propylene oxide/Epon 1:2	4 h	RT
Epon	4 h	RT

The samples were moved into casts and embedded in epon. The polymerization of the epon took place at 60 °C for 24 h.

2.2.4.2. Preparation of semithin slices

The embedded samples were trimmed with a shaper and sectioned into semithin slices (0.5 µm) with a microtome (Ultracut S). The slices were transferred onto object slides and dyed with freshly prepared and filtrated methylene-azure-II dye for 1 min at 60 °C, following the protocol of Richardson et al. (1960). The dye was washed away with distilled water and the object slides were dried for 10 min at 60 °C and covered with coverslips, using Eukitt® as mounting medium.

2.2.4.3. Light microsopy

Histological characteristics in the peripheral nerve, such as tomacula and their possible preforms (myelin invaginations) were quantified on pictures taken of the dyed semithin samples of the *N. ischiadici* using an optical microscope (Axiophot, Zeiss) with a digital camera (Kappa). The samples were magnified 100x. The processing of the pictures followed with Adobe Photoshop CS5. Plugin Cell Counter (ImageJ) was used to count the total amount of axons in each *N. ischiadicus*, as well as the amount of tomacula and myelin invaginations. The characterization of the axons followed in a blinded manner.

2.2.5. Electrophysiological measurements

The electrophysiological measurements were performed by Dr. Robert Fledrich in a blinded manner. Hence the genotype of the animals was not known to the examiner. Compound muscle action potentials (CMAPs), nerve conduction velocities (NCVs) and distal motor latencies (DMLs) were recorded using fine subcutaneous needle electrodes and the results were documented with a Jaeger-Toennis Neuroscreen instrument. The CMAPs were evoked through electrical stimuli of 0.1 ms of the tail nerve. The muscle responses were recorded through electrodes, and the amplitudes between the lowest and the highest values were documented. NCVs were calculated from the latency difference between the CMAPs after successive proximal stimulation at two sites 2 cm apart. CMAP reflects the degree of axonal degeneration and NCV is a measure for myelin defects. In general, a normal NCV and a decreased CMAP suggest a purely axonal neuropathy, while a slowing of the NCV implies a demyelinating neuropathy (Dyck and Thomas 2005). DMLs were recorded as the interval between a stimulation of a compound muscle and the observed response (ms). Conduction block (CB) was not provoked but its spontaneous presence, defined by > 50 % reduction of CMAP amplitudes between proximal and distal sites of stimulation was calculated. CB indicates a failure of the action potential propagation along the axon as a consequence of demyelination (Kaji 2003). The data acquired from the electrophysiological measurements, performed by the colleague, were used by the author for the statistical analyses and their graphical representation.

2.2.6. Statistical analysis

The data for the statistical analyses were sorted and processed with Excel 2010 and analyzed with GraphPad Prism® 5.0. The results were evaluated with an unpaired Student´s *t*-test, using a significance level of $p < 0.05$. The mean and standard deviation (SD) is shown in the figures.

3. Results

3.1. Identification of an effective progesterone dosage on Pmp22 expression after short-term application on HNPP mice

The short-term pilot study was performed with two different dosages of progesterone. The amount of *Pmp22* mRNA in the *N. ischiadici* was determined with real-time PCR, in which the expression of each sample was normalized to the mean of the best stable housekeeping genes Rps20 and Rplp0.

The HNPP mice (*Pmp22*$^{+/-}$) showed, in accordance with the patient situation, a significantly reduced level of *Pmp22* expression compared to the wild type controls. A therapy at 10 mg/kg bw of progesterone for nine days did not alter the lower expression level. However, a significant increase in *Pmp22* expression towards wild type levels was found in the HNPP mice at 40 mg/kg bw of progesterone (Figure 7). This dosage was used in the subsequent long-term therapy studies.

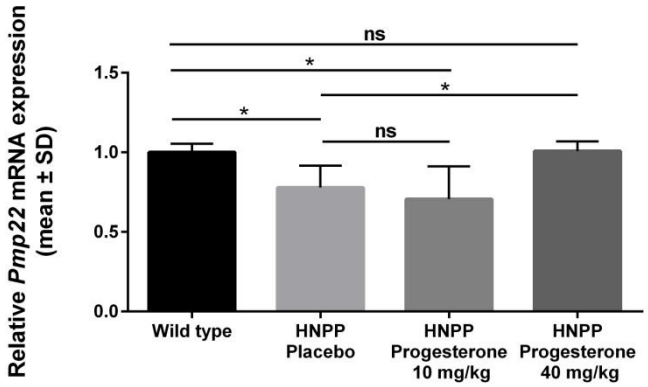

Figure 7: Pilot study. Subcutaneous injections of progesterone were given every second day for nine days. The HNPP mice expressed a lower amount of *Pmp22* than their wild type littermates ($p < 0.05$. Wild type: n = 4, mean = 1.0 ± 0 .05; placebo: n = 7, mean = 0.78 ± 0.14). An increase in the expression was observed after injections of 40 mg/kg bw progesterone ($p < 0.05$, n = 3, mean = 1.01 ± 0.06) but not after that of 10 mg/kg bw ($p > 0.05$, n = 6, mean = 0.71 ± 0.21).

3.2. Time-dependent normalization of Pmp22 expression levels in HNPP mice after long-term therapy with progesterone

The mean of the best stable housekeeping genes cyclophilin, β-actin, Rplp0 and Rps20 was used for normalization in the two long-term therapy studies. Again *Pmp22* mRNA levels were significantly lower in the HNPP mice compared to their wild type littermates at the age of 90 days, as well as 180 days. The long-term therapy with progesterone at 40 mg/kg bw was effective in significantly increasing the expression of *Pmp22* towards wild type levels after a 2-month treatment period (P90) (Figure 8A). However, no significant effects were found in the *Pmp22* expression after a 5-month progesterone therapy (P180) (Figure 8B).

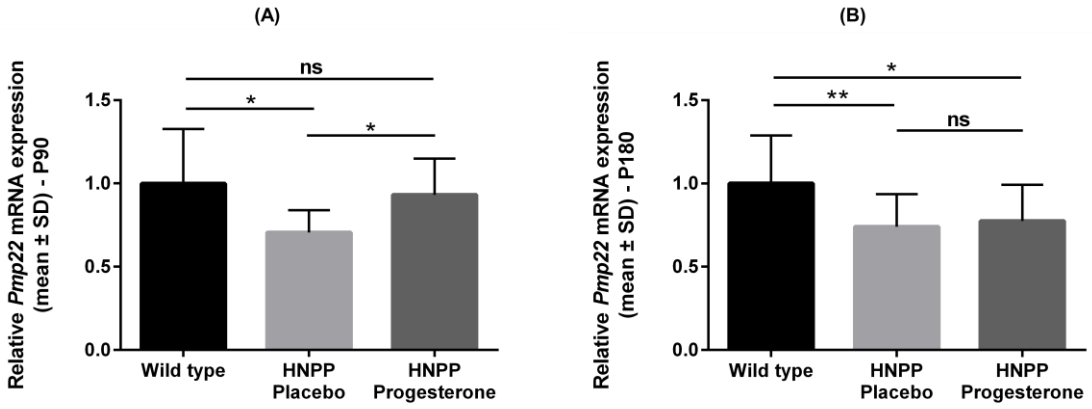

Figure 8: Relative *Pmp22* expression after long-term treatment. (A): 2-month study. The placebo-treated HNPP mice showed a lower expression level of *Pmp22* than the wild type controls ($p < 0.05$. Wild type: n = 11, mean = 1.0 ± 0.33; placebo: n = 7, mean = 0.71 ± 0.13). The progesterone-treated HNPP mice expressed significantly more *Pmp22* ($p < 0.05$, n = 12, mean = 0.93 ± 0.22) than the placebo-treated ones. (B): 5-month study. The placebo-treated HNPP mice expressed less *Pmp22* than the wild types ($p < 0.01$. Wild type: n = 11, mean = 1.0 ± 0.29; placebo: n = 16, mean = 0.74 ± 0.19). No significant increase in the expression level was seen after five months of treatment with progesterone ($p > 0.05$, n = 14, mean = 0.78 ± 0.22).

3.3. Pmp22 and Krox-20 expression levels correlate in HNPP mice after treatment with progesterone

The placebo-treated HNPP mice and the wild type controls showed no significant difference in the expression of *Krox-20* after the 2-month study. However, in accordance with the results obtained with *Pmp22*, *Krox-20* mRNA expression was significantly increased in

the HNPP mice treated with progesterone for two months at 40 mg/kg bw (Figure 9A), and no effect on *Krox-20* was observed in the mice treated for five months (Figure 9B). At this time point the expression of *Krox-20* was found to be significantly lower in the placebo-treated HNPP mice compared to the wild types.

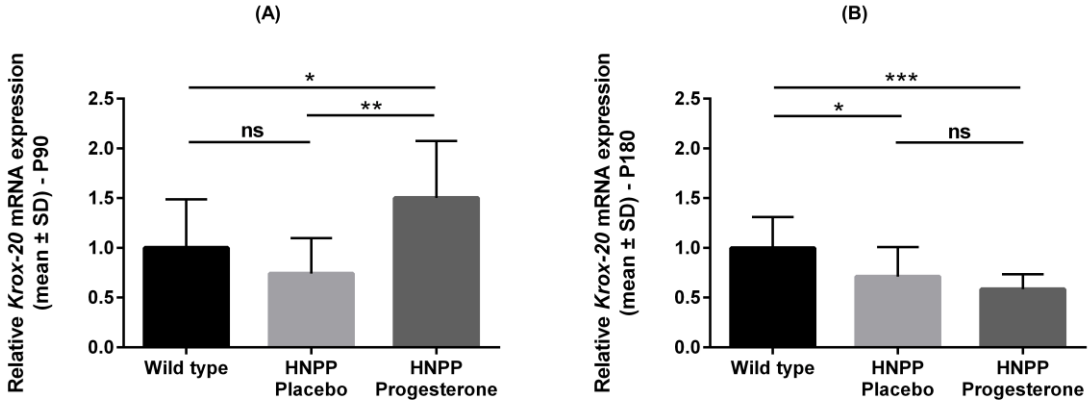

Figure 9: Relative *Krox-20* expression after long-term treatment. (A): 2-month study. No significant difference in the expression levels between the wild types and the placebo-treated HNPP mice was observed ($p > 0.05$. Wild type: $n = 11$, mean = 1 ± 0.49; placebo: $n = 7$, mean = 0.74 ± 0.36). The progesterone-treated HNPP mice expressed significantly more *Krox-20* than the placebo-treated ones ($p < 0.01$, $n = 12$, mean = 1.50 ± 0.57). (B): 5-month study. The placebo-treated HNPP mice expressed less *Krox-20* than the wild types ($p < 0.05$. Wild type: $n = 11$, mean = 1.0 ± 0.31, placebo: $n = 16$, mean = 0.71 ± 0.30). No significant increase in the expression level was seen after five months of treatment with progesterone ($p > 0.05$, $n = 13$, mean = 0.59 ± 0.15).

The correlation between the expression levels of *Pmp22* and *Krox-20* was observed by plotting the *Pmp22* expression of each HNPP mouse against its *Krox-20* expression. The results showed significant positive correlations in the animals treated for two months (Figure 10A) and for five months (Figure 10B) (placebo- and progesterone-treated HNPP mice plotted together).

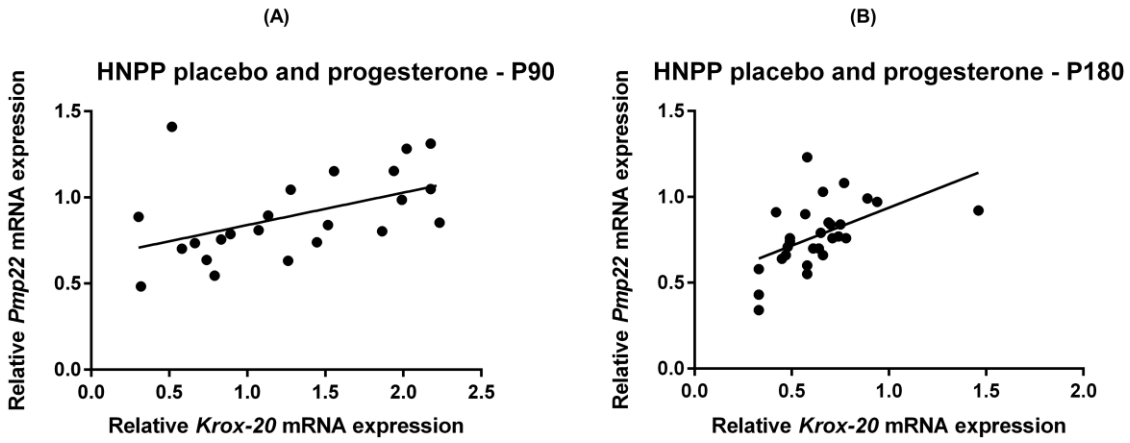

Figure 10: Expression levels of *Pmp22* and *Krox-20* plotted against each other. A significant positive correlation between the expression levels of *Pmp22* and *Krox-20* was found in the placebo- and progesterone-treated HNPP mice after the 2-month study ($p < 0.05$. Placebo: n = 7, progesterone: n = 16, $r^2 = 0.23$) (A), as well as after the 5-month study ($p < 0.01$. Placebo: n = 15, progesterone: n = 13, $r^2 = 0.27$) (B).

3.4. No axonal loss detected in HNPP mice

The total number of myelinated axons was quantified from the *N. ischiadici* of the mice and was not found to differ between any of the groups (Figure 11A-B).

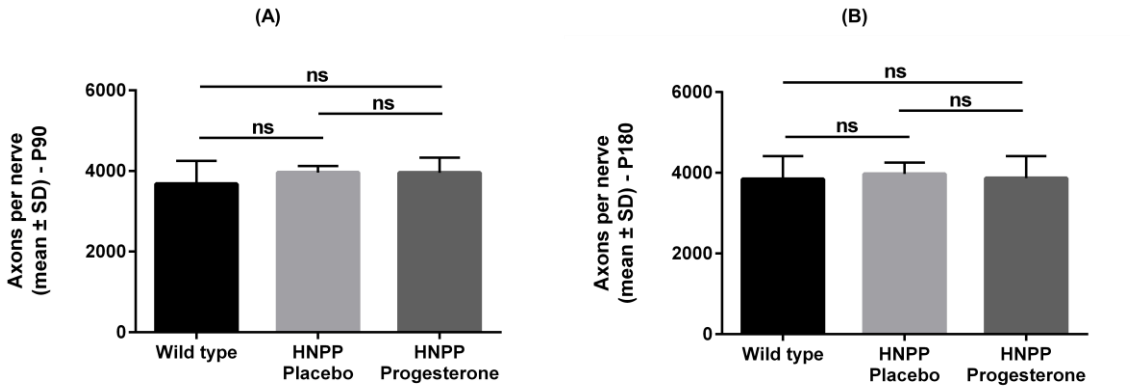

Figure 11: Total amount of myelinated axons per nerve (*N. ischiadicus*). The number of myelinated axons was counted from pictures of nerve cross sections obtained by light microsopy. No significant difference ($p > 0.05$) existed between the wild types, the placebo-treated HNPP mice and the progesterone-treated HNPP mice after the 2-month study (wild type: n = 9, mean = 3679 ± 573; placebo: n = 7, mean = 3961 ± 163; progesterone: n = 15, mean = 3959 ± 376) (A), nor after the 5-month study (wild type: n = 5, mean 3844 ± 567; placebo: n = 15, mean 3971 ± 281; progesterone: n = 13, mean = 3869 ± 542) (B).

3.5. HNPP mice show more tomacula and myelin invaginations and the situation is not corrected after progesterone therapy

The peripheral nerves of *Pmp22*$^{+/-}$ mice show typical characteristics, such as tomacula and myelin invaginations (Adlkofer et al. 1997). The amount of these pathological formations was quantified from *N. ischiadici*. Normal axons and tomacula are depicted in Figure 12. The HNPP mice showed a significantly larger amount of tomacula (Figure 13) and abnormal myelin invaginations (Figure 14) than the wild type animals and the amount of these myelin alterations increased significantly with age. No therapy effect concerning these features was observed after progesterone therapy.

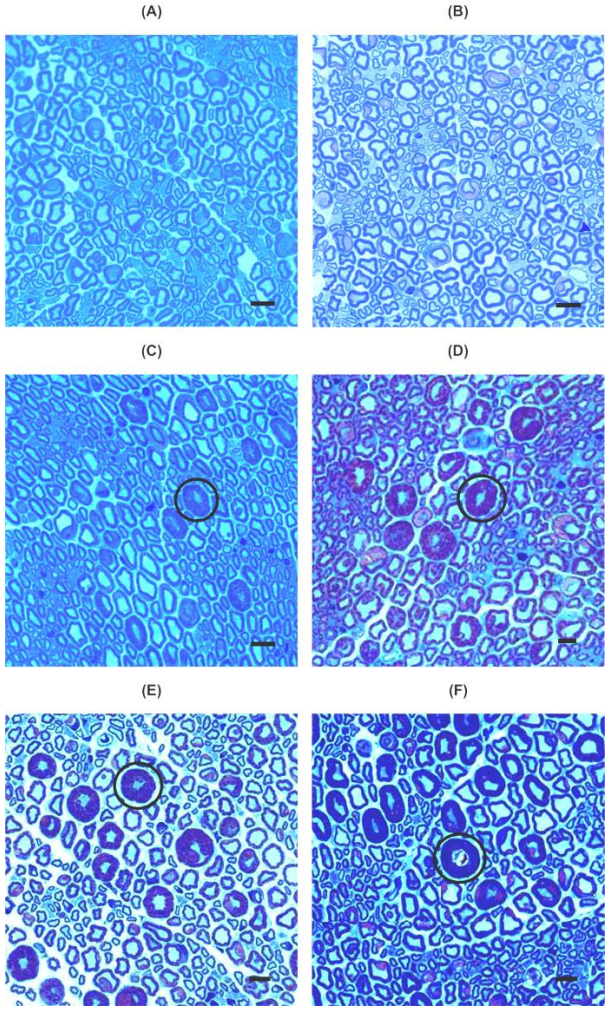

Figure 12: Sciatic nerve cross sections of wild type and HNPP mice of different ages (methylene-azure-II dye). Pictures obtained by light microsopy. Normal axons of wild type mice at P90 (A) and at P180 (B). Normal axons and tomacula (encircled) of placebo-treated HNPP mice at P90 (C) and at P180 (D) and of progesterone-treated HNPP mice at P90 (E) and at P180 (F). Scale bar: 10 µm.

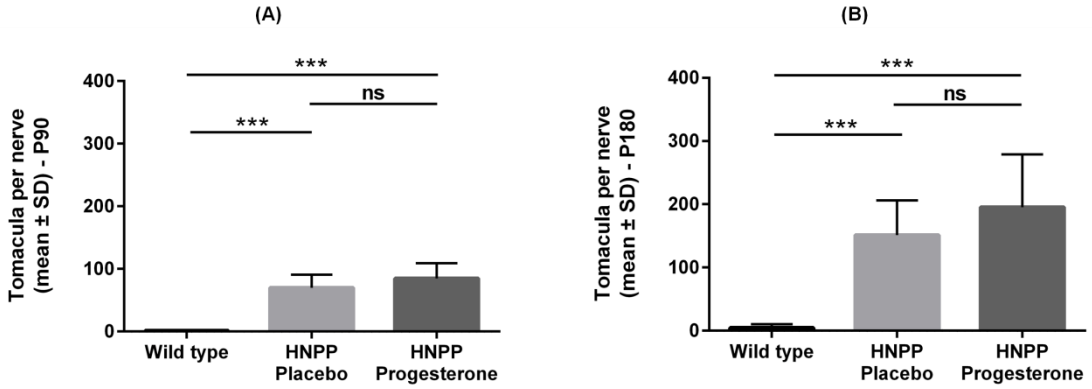

Figure 13: Total amount of tomacula per nerve (*N ischiadicus*). The number of tomacula was counted from pictures of nerve cross sections obtained by light microsopy. The HNPP mice showed a significantly larger amount of tomacula than the wild types. No significant difference in the numbers was found between the placebo- and progesterone-treated HNPP mice. (A): 2-month study (wild type vs. placebo: $p < 0.001$. Wild type: n = 9, mean = 1.0 ± 1.1; placebo: n = 7, mean = 69.9 ± 21.1; progesterone: n = 15, mean = 84.9 ± 24.2). (B): 5-month study (wild type vs. placebo: $p < 0.001$. Wild type: n = 5, mean 4.4 ± 5.9; placebo: n = 15, mean = 151.2 ± 55.0; progesterone: n = 13, mean = 195.2 ± 83.0). The amount of tomacula increased as the animals grew older ($p < 0.01$).

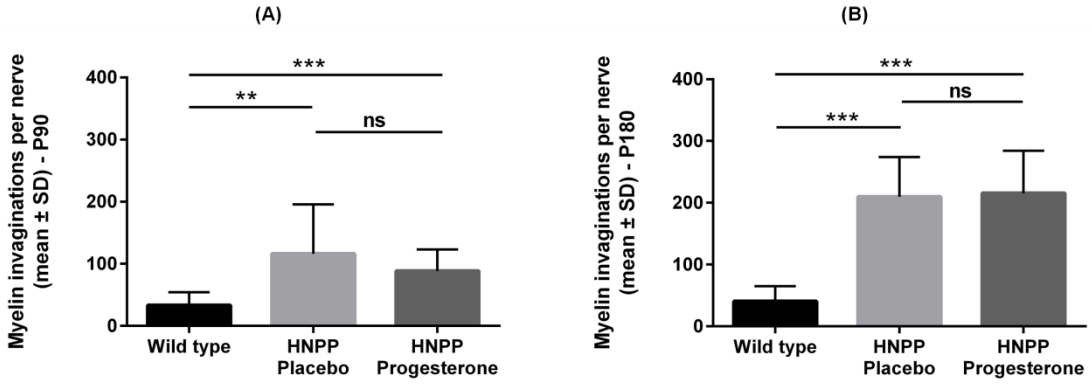

Figure 14: Total amount of myelin invaginations per nerve (*N. ischiadicus*). The number of myelin invaginations was counted from pictures of nerve cross sections obtained by light microsopy. The HNPP mice showed a significantly larger amount of myelin invaginations than the wild types. No significant difference in the numbers was found between the placebo- and progesterone-treated HNPP mice. (A): 2-month study (wild type vs. placebo: $p < 0.01$. Wild type: n = 9, mean 33.0 ± 21.2; placebo: n = 7, mean = 116.0 ± 79.9; progesterone: n = 15, mean = 88.4 ± 34.8). (B): 5-month study (wild type vs. placebo: $p < 0.001$. Wild type: n = 5, mean = 40.4 ± 24.8; placebo: n = 15, mean = 209.7 ± 64.4; progesterone: n = 13, mean = 215.5 ± 68.6). The amount of myelin invaginations increased as the animals grew older ($p < 0.01$).

3.6. Electrophysiological studies

Significantly reduced CMAPs and NCVs and increased DMLs were observed in the HNPP mice compared to the wild types. No beneficial therapy effects regarding these features were obtained with progesterone (Figure 15A-H). CBs were occasionally observed in HNPP mice from both the placebo- and the progesterone-treated group after the 2-month study (P90) but in neither group after the 5-month study (P180) (Figure 15I-J).

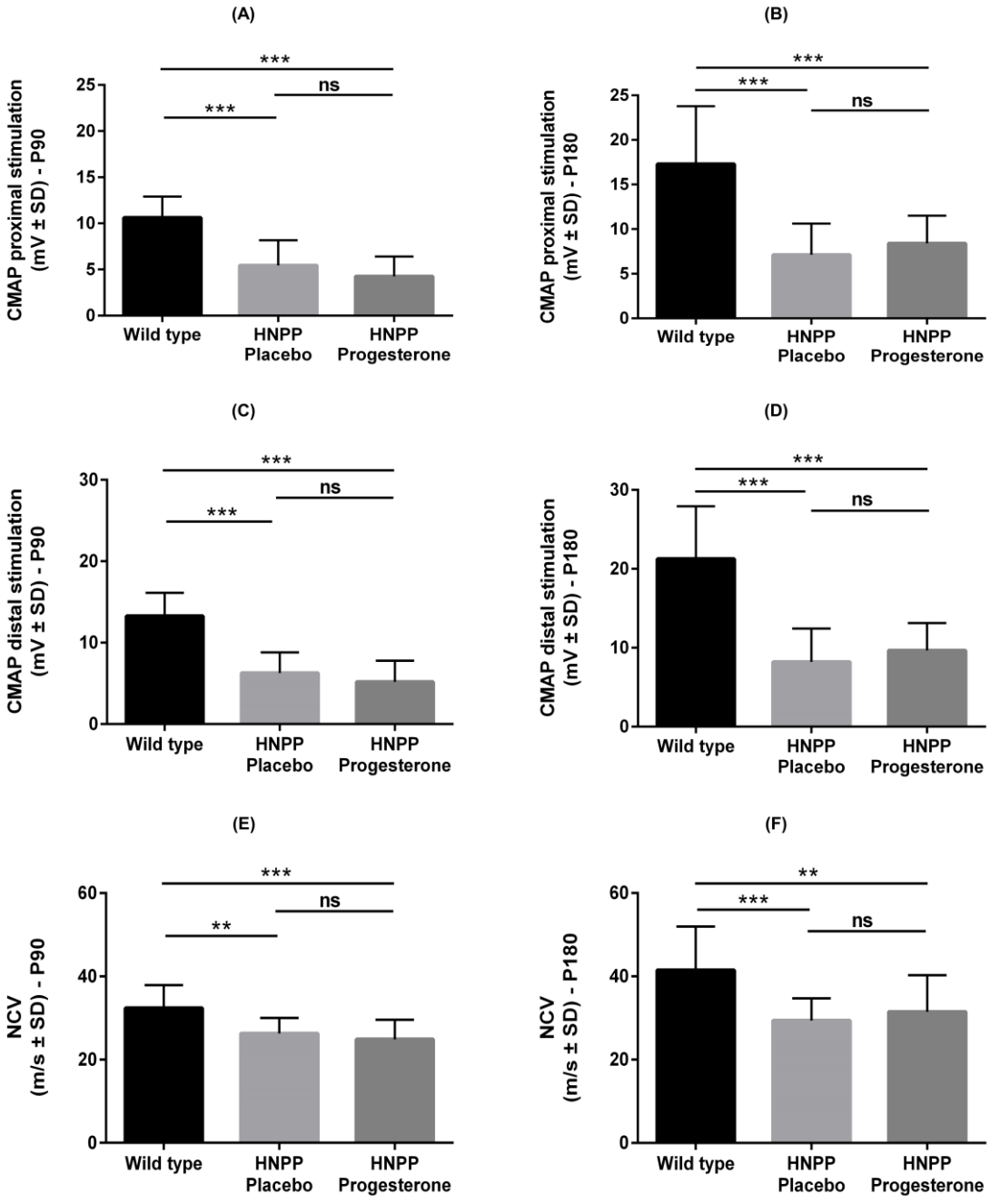

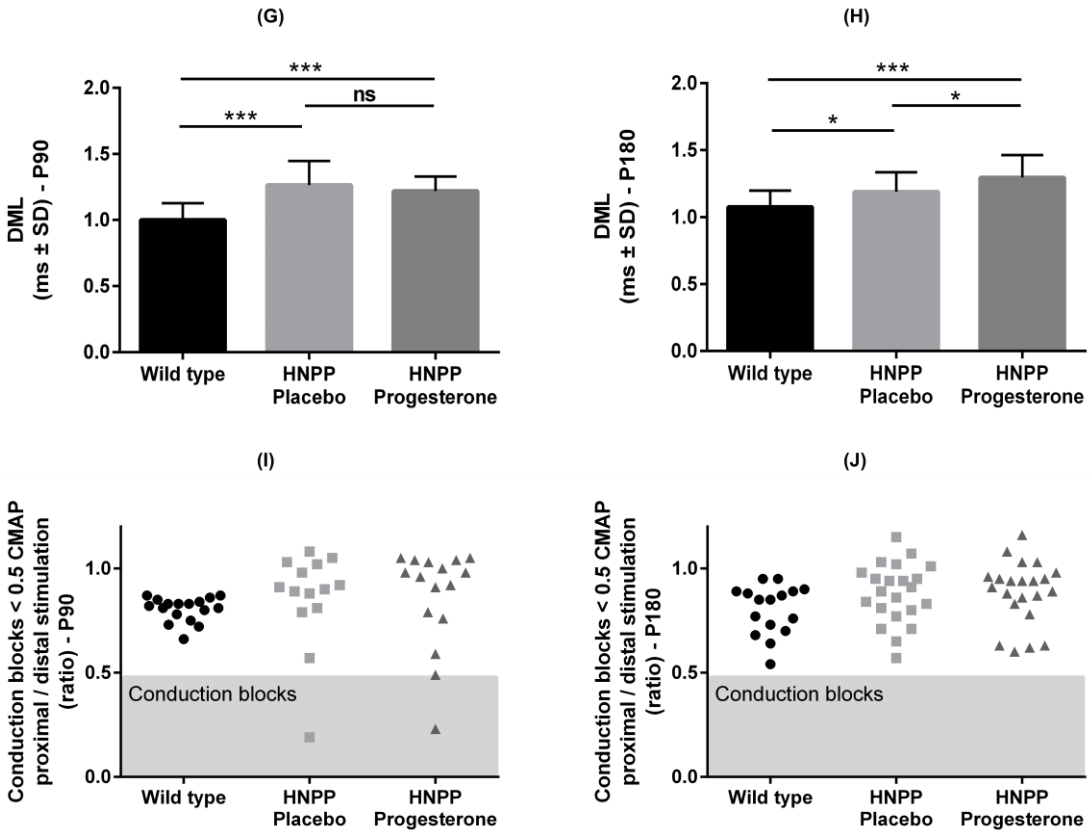

Figure 15: Electrophysiological studies performed on HNPP and wild type mice. Decreased proximal and distal CMAPs and NCVs ($p < 0.01$) were observed in the placebo-treated HNPP mice compared to the wild type controls after the 2- and the 5-month studies. No therapy effect was found after treatment with progesterone (A-F). The DMLs were significantly increased in the placebo-treated HNPP mice and a further increase was observed in the progesterone-treated group after the 5-month study ($p < 0.05$) (G-H). CB was observed in one mouse from the placebo-treated group (CMAP proximal/CMAP distal = 0.19) and in two mice from the progesterone-treated group (CMAP proximal/CMAP distal = 0.23 and 0.49) after the 2-month-study. No CB was detected after the 5-month study.

Proximal CMAP 2-month study: wt: n = 17, mean = 10.62 ± 2.28; placebo: n = 14, mean = 5.46 ± 2.73; progesterone: n = 16, mean = 4.27 ± 2.14. Proximal CMAP 5-month study: wt: n = 16, mean = 17.29 ± 6.48; placebo: n = 22, mean = 7.11 ± 3.49; progesterone: n = 22, mean = 8.41 ± 3.10. Distal CMAP 2-month study: wt: n = 17, mean = 13.26 ± 2.86; placebo: n = 14, mean = 6.27 ± 2.55; progesterone: n = 16, mean = 5.20 ± 2.60. Distal CMAP 5-month study: wt = 16, mean = 21.25 ± 6.69; placebo: n = 22, mean = 8.22 ± 4.21; progesterone: n = 22, mean = 9.67 ± 3.47. NCV 2-month study: wt: n = 17, mean = 32.39 ± 5.48; placebo: n = 14, mean = 26.26 ± 3.76; progesterone: n = 16, mean = 24.89 ± 4.67. NCV 5-month study: wt: n = 16, mean = 41.45 ± 10.53; placebo: n = 22, mean = 29.36 ± 5.34; progesterone: n = 22, mean = 31.45 ± 8.82. DML 2-month study: wt: n = 17, mean = 1.00 ± 0.13; placebo: n = 14, mean = 1.26 ± 0.18; progesterone: n = 16, mean = 1.22 ± 0.11. DML 5-month study: wt: n = 16, mean = 1.08 ± 0.12: placebo: n = 26, mean = 1.19 ± 0.15; progesterone: n = 21, mean = 1.30 ± 0.17. CB 2-month study: wt: n = 17; placebo: n = 14; progesterone: n = 16. CB 5-month study: wt: n = 16: placebo: n = 22; progesterone: n = 22.

3.7. No side-effects on long-term body weight increase after progesterone therapy

The weight of the mice was controlled regularly during the long-term studies in order to detect a possible side-effect on the body weight increase during and after therapy with progesterone. No significant difference was found between the progesterone-treated HNPP animals and the placebo-treated HNPP controls, nor between these mice and the wild types (Figure 16).

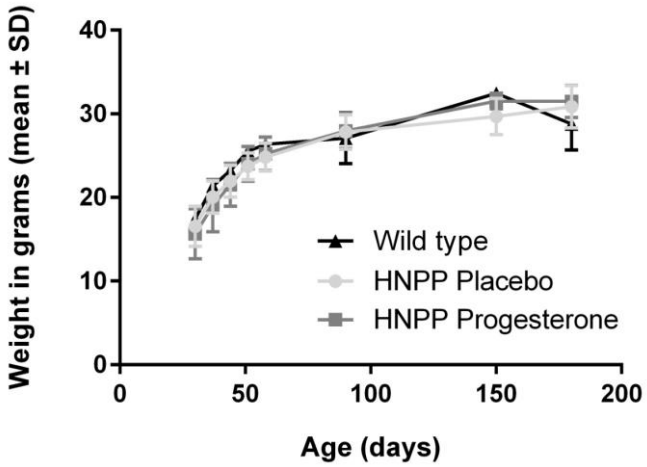

Figure 16: Weight curve. The mice were weighed regularly. No significant difference in the weights (g) was found between any of the groups at any time point ($p < 0.05$). P30: wild type: n = 1, mean = 17.46 ± 0.00; placebo: n = 25, mean = 16.54 ± 2.42; progesterone: n = 30, mean = 15.64 ± 3.02. P90: wild type: n = 12, mean = 27.10 ± 3.03; placebo: n = 25, mean = 27.83 ± 2.09; progesterone: n = 30, mean = 27.87 ± 2.10. P180: wild type: n = 4, mean = 28.78 ± 3.11; placebo: n = 16, mean = 30.85 ± 2.53; progesterone: n = 12, mean = 31.49 ± 1.95.

3.8. Mean progesterone dosage delivered to HNPP mice decreases with time

The body mass of the mice increased as they grew older, and since the amount of progesterone was released from the pellets in a constant manner, the dosage of progesterone delivered decreased following a reverse pattern, thus being lower than the aimed dosage of 40 mg/kg bw, as seen in Figure 17.

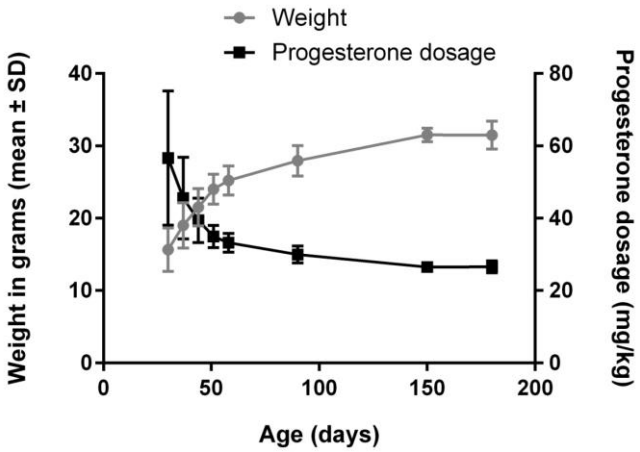

Figure 17: Weight- and dosage curves. The dosage of progesterone (mg/kg bw) decreased as the animals gained weight (g) while growing older. The curve with the dots depicts the weights of the mice at time points between 30-180 days (x-axis). The curve with the squares represents the dosage of progesterone (mg/kg bw) obtained at each time point. Wild type: n = 1-12; placebo: n = 17-25; progesterone: n = 12-13.

4. Discussion

Two goals were set for the thesis: 1) the comparison of the HNPP mouse model at the level of *Pmp22* expression, axon and myelin pathology, as well as electrophysiological characteristics to the very limited amount of published data regarding these features, and using the results of the study to evaluate the similarity of the model to human HNPP patients and thus its suitability as a reliable disease model. This is important in the light of the fact that when creating a mouse model and building up a colony that will breed, there is a risk of loss of the disease phenotype of interest (Perrin et al. 2014). 2) To study whether an increase in *Pmp22* expression can be achieved through a therapy with progesterone, with the potential of offering a causal pharmacological therapy option in HNPP.

4.1. Pmp22 expression, histological phenotype and electrophysiological features of the HNPP mouse model correlate to a great degree to that of human patients

4.1.1. Decreased *Pmp22* expression in HNPP mice

The transgenic mouse model for HNPP, lacking one functioning allele of the *Pmp22* gene, is expected to express decreased levels of *Pmp22*, which was confirmed in this thesis. The expression level remained stable at the time points of P90 (0.71-fold of wild type controls) and P180 (0.74-fold of wild type controls). Since the rodent model, as well as the human patients, has one functioning allele of the *Pmp22* gene, one could assume an expression level of 0.5. It is possible that the mouse model has certain limitations and that the disease is not as marked in the rodents as it is in the human HNPP patients.

4.1.2. Increased amount of tomacula and myelin invaginations in HNPP mice

The number of myelinated axons did not differ in the three groups of study animals (wild type controls, placebo-treated HNPP mice and progesterone-treated HNPP mice) at neither of the time points of P90 and P180 in this study (Figure 11). However, the number of tomacula and myelin invaginations was significantly higher in the HNPP mice and increased with age (Figures 13-14). The presence of tomacula is in line with previous data from $Pmp22^{+/-}$ mice but a new observation, not seen before when comparing mice of the

age of 5, 10 and 15 months (Adlkofer et al. 1997), was that the number of hypermyelinated axons increased during aging. Even the number of myelin invaginations increased with age.

Semithin sections of sural nerve biopsies from HNPP patients reveal abnormalities of the myelin sheath. The characteristic picture consists of fibres with a thin myelin sheath and myelin thickenings with tomaculous and outfolding-like features. Moreover, moderate axonal loss and mild reduction of myelinated fibre density and axonal degeneration is observed (Luigetti et al. 2014). Tomacula are also visible in teased fibres preparations (Behse and Buchtal 1971; Koike et al. 2005; Luigetti et al. 2014), as are signs of segmental de/remyelination and increased axonal degeneration (Koike et al. 2005). Therefore the HNPP mouse model mimics histological features in human patients regarding the presence of tomacula.

4.1.3. Presence of various electrophysiological abnormalities in HNPP mice

Mild alterations in electrophysiological features (reduction of the M-response) were detected in a previous study on *Pmp22*$^{+/-}$ mice of 12-14 months of age. However, no changes in NCVs, motor and mixed afferent latencies, F-wave latencies and duration of M- and F-responses were seen. No abnormalities were detectable at the earlier time point of 10 weeks (Adlkofer et al. 1995). In another study, induced CB has been demonstrated to occur more rapidly in *Pmp22*$^{+/-}$ mice than in wild types (Bai et al. 2010). In the study performed for this thesis, distal and proximal CMAPs, NCVs and DMLs were measured in 90- and 180- day old animals. The HNPP mice displayed significantly reduced CMAPs and NCVs and increased DMLs compared to the wild type controls. CB was not provoked in the present study but its spontaneous presence was occasionally observed in HNNP mice at P90.

The neuropathy in humans shows great heterogeneity regarding its clinical and electrophysiological manifestations (Beydoun and Cho 2013), but patients are mostly, whether symptomatic or not (Infante et al. 2001), reported to display characteristic alterations, including prolongation of DMLs (Li et al. 2002; Pou Serradell et al. 2002; Yurrebaso et al. 2014), especially of the median and peroneal nerves (Li et al. 2002), slightly reduced NCVs with slowing of motor nerve conduction velocities, mostly at entrapment sites (Gouider et al. 1995; Mouton et al. 1999; Infante et al. 2001; Li et al. 2002; Pou Serradell et al.2002; Yurrebaso et al. 2014) and occasional CBs (Pou Serradell et al. 2002; Yurreba-

so et al. 2014). Sensory NCVs and sensory nerve action potentials amplitudes are often reduced (Li et al. 2002; Hong et al. 2003). A reduction in CMAP amplitudes can be present and has been documented to increase during aging in nerves vulnerable to entrapment (Koike et al. 2005), seen as a sign of slowly progressive axonal loss (Herskovitz et al. 2010). The most affected nerves for electrophysiological alterations seem to be the motor and sensory ulnar nerve, the deep fibular nerve, the sensory and motor median nerve, the sural nerve and the superficial radial nerve (de Oliveira et al. 2016).

4.2. A time-dependent normalization of Pmp22 expression without positive histological or electrophysiological effects was obtained in the HNPP mouse model after therapy with progesterone

The studies were performed on male HNPP and wild type mice in order to avoid the cyclic fluctuations of progesterone in female mice. The application of progesterone and placebo followed with subcutaneous injections in the pilot study and with subcutaneous pellets in the two long-term studies of two and five months. In the doctoral thesis of Dr. med. Thomas Prukop it was shown that progesterone is released from the pellets in a constant manner according to the information given by the manufacturer (Prukop 2008). Thus, the amount of substance released per kg/bw decreases as the animal gains weight during its development from a pup to an adult. This is visualized in Figure17 where the ratio between body weight (g) and progesterone dosage (mg/kg bw) is depicted.

4.2.1. Increased *Pmp22* gene expression after therapy with progesterone

In the present study it was shown that although HNPP mice express decreased levels of *Pmp22*, the expression rate can, however, be altered. In a short dosage finding pilot study that lasted for nine days, as well as in a long-term study of two months, a therapy with progesterone significantly increased the level of *Pmp22* to wild type levels. Hence, the study provides proof of principle for *Pmp22* normalization by a pharmacological drug therapy.

Interestingly, the increased *Pmp22* expression level could no longer be observed in animals after a treatment of five months. A range of factors may play a role in this process. This could be due to an insufficient amount of progesterone reaching its target as the concentration of the substance decreases as the weight of the animal increases with aging. The dos-

age of progesterone had a mean of 56.6 ± 18.6 mg/kg bw in the beginning of the study (P30) and decreased continuously, having a mean of 30.0 ± 2.4 mg/kg bw as the 2-month study ended (P90) and only 26.6 ± 1.7 mg/kg bw at the end of the 5-month study (P180). Another important observation is the local reaction of the subdermal tissue to the implanted pellet. A pellet rejection was observed in many of the animals from the 5-month study, possibly due to the longer time that the pellet stayed implanted, and/or the larger size of the second implanted pellet. It seems plausible that a capsulation and a rejection of the pellet impair blood circulation in that area, leading to a decreased amount of progesterone reaching the circulation and its target tissues. Considering both these observations together; the effects of combined rejection of the pellet and the lower dosage of progesterone as the weight increases with time, one may hypothesize that this contributed to the low expression level of *Pmp22* in HNPP mice after five months of treatment.

KROX-20 is a transcription factor stimulated by progesterone (Guennoun et al. 2001; Mercier et al. 2001; Magnaghi et al. 2007) and an inductor of *PMP22* expression (Nagarajan et al. 2001; Le et al. 2005). This study supports both of these statements. The expression of *Krox-20* increased in the HNPP mice after treating them for two months with progesterone and correlated positively with the expression of *Pmp22*. Thus, stimulation of *Pmp22* through KROX-20 seems plausible. An increased expression level of *Krox-20* was, however, not seen after a 5-month treatment with progesterone. This observation was in line with the unaltered expression of *Pmp22* after the long-term treatment.

4.2.2. No changes in histological features after therapy with progesterone

No effects regarding the structural changes of axons in the HNPP mice were seen after treatment with progesterone; the amount of tomacula and myelin invaginations remained unchanged. It is possible that the upregulated *Pmp22* mRNA expression, in the case of the 2-month study, is not sufficient to counteract the formation of these structures long-term, and a certain threshold level has to be reached for this to take place. In the case of CMT1A, a threshold for therapeutic effectiveness by downregulating *Pmp22* overexpression via a progesterone antagonist in rats has been discussed (Meyer zu Hörste et al. 2007).

4.2.3. No changes in electrophysiological parameters after therapy with progesterone

No positive therapy effect regarding the electrophysiological findings was seen after treatment with progesterone. The CMAPs and NCVs remained reduced and the DMLs were still prolonged. Reduced NCVs not being improved by progesterone may reflect the unaffected myelin pathology as shown by the quantification of tomacula and invaginations, and missing effects on the axonal number in the peripheral nerve may explain why CMAPs were not affected by progesterone therapy in the HNPP mice. On the other hand, CMAPs were obviously reduced in the HNPP mice although no axonal degeneration was present. Therefore, some axonal damage must be present in the HNPP mice, which however could not be demonstrated by the quantification of total axonal number itself. DML abnormalities are currently not well understood in hereditary peripheral neuropathies, however, a relation to the end terminal transduction via the neuromuscular junction is discussed (Prukop et al. 2017). Although the analysis showed significantly increased DMLs in the HNPP mice, the interpretation remains limited due to missing histological correlation data with neuromuscular junctions.

4.3. Suggestions for optimizing future therapy studies in HNPP mice

Data obtained from the performed study, as well as challenges met during it, serve as valuable information for further therapy studies in the HNPP mouse model. It was shown that these mice do show pathological features known to the human patients, and that an alteration of *Pmp22* expression can in general be gained though treatment with progesterone. Regarding the upregulation of *Pmp22* using progesterone as a therapeutic substance a few alterations and new approaches may be applied in future studies. For one, a study on a larger scale, increasing the n-number, would reflect the mean more reliably.

The difficulty with the decreasing amount of progesterone released as the animals gain weight could be tackled using another form of application. Application of the therapeutic substance by mixing it in the food allows the optimization of the dosage at any desired time point. It is an option widely used, although one can never be certain of the exact amount of food consumed by the animal. Nevertheless, the problem with pellet capsulation and rejection could be overcome by applying progesterone in the food. Another way of

controlling the dosage is by applying progesterone through subcutaneous injections. Experience from the pilot study taught, however, that regular injections in the subcutis lead to an induration of the skin, making it more challenging to perform the injections long-term.

The dosage of progesterone must be carefully optimized; using a dosage that is not only sufficient to stimulate the expression but large enough to achieve a normalization to wild type levels, while at the same time not inducing an over-expression comparable to the CMT1A phenotype.

In the case of CMT1A, a disease caused by *PMP22* gene duplication, downregulating the gene expression is the aim, and several compounds impacting *Pmp22* have been tested both in vitro and or in vivo. Onapristone (Chabbert-Buffet et al. 2005), a progesterone receptor antagonist, has been shown to reduce *PmpP22* mRNA overexpression and to eliminate the neuropathic phenotype when given to early postnatal CMT1A rats (Sereda et al. 2003), as well as to older CMT1A rats (Meyer zu Hörste et al. 2007). PXT3003, a combination of three drugs (baclofen, naltrexone and sorbitol) has been shown to exert its effect on CMT1A in cell cultures, in the rodent model for the disease (Chumakov et al. 2014), as well as in clinical trials (Attarian et al. 2014). It was shown to lower *Pmp22* overexpression and to improve myelination in vitro and in vivo in the transgenic rats and to ameliorate the clinical phenotype in the rodents. The three molecules were separately able to increase myelination as well but had a greater impact when used in combination (Chumakov et al. 2014). Overexpressed neuregulin-1 (NRG1), a recombinant human growth factor which controls myelin thickness, has been shown to counter the effect of *Pmp22* overexpression in early postnatal development in a rat model, although not by reducing the overexpression itself. This appears to occur through modulation of downstream signaling through kinases and is shown to improve the differentiation of Schwann cells (Fledrich et al. 2014). Protein kinase C (PKC) modulator bryostatin has been shown to lower *Pmp22* expression by first activating PKC and then depressing its activity on a long-term basis (Inglese et al. 2014). Other PKC modulating bryostatin-like molecules have also been identified (Ruan and Zhu 2012).

An interesting question is if substances that target the molecules mentioned above or other molecules that regulate the activity of *Pmp22* expression or counter the effects of *Pmp22* underexpression could be applied in the case of the HNPP transgenic model. Onapristone works by antagonizing the progesterone receptor (Sereda et al. 2003). Baclofen targets the

GABA-B receptor, Naltrexone binds to opioid receptors and sorbitol may bind muscarinic acetylcholine G-protein coupled receptors or acts as a chaperone. How PXT-3003, the combination of baclofen, naltrexon and sorbitol, exerts its effect on *Pmp22* downregulation is still not fully understood (Ekins et al. 2015). NRG1 counters the effect of *Pmp22* (Fledrich et al. 2014) and bryostatin exerts its downregulating effect on *Pmp22* expression (Inglese et al. 2014) through kinases (Fledrich et al. 2014; Inglese et al. 2014).

In fact, other receptors and substances have been shown to play a role in the activation of *Pmp22* expression. *Pmp22* expression is not only stimulated through activation on PR, but also through the interaction with non-classical steroid receptors, such as the GABA-A receptor (Melcangi et al. 2005), and this activation leads to a higher level of *Pmp22* (Caruso et al. 2008). Both the sciatic nerve of adult male rats and Schwann cells express several subunits of this receptor (Melcangi et al. 1999b; Melcangi et al. 2005). Schwann cells are able to actively convert progesterone into dihydroprogesterone (DHP) through the action of the 5α-reductase and then through the action of the 3α-reductase into tetrahydroprogesterone (THP) (Melcangi et al. 1990; Melcangi et al.1998a; Yokoi et al. 1998) and these enzymes are present both in the CNS and in the PNS (Celotti et al. 1992; Melcangi et al. 1999b). THP is not able to directly bind to the PR, unless it is converted back to DHP, but interacts directly with some components of the GABA-A receptor (Rupprecht et al. 1993; Rupprecht et al. 1996; Melcangi et al. 1999b; Melcangi et al. 2001). The peripheral nerves of aged male rats show morphological changes and decreased levels of *Pmp22* (Melcangi et al. 1998b; Melcangi et al. 1999a; Azcoitia et al. 2003; Melcangi et al. 2003). THP has been demonstrated to increase the amount of *Pmp22* in Schwann cell cultures, as well as in vivo in the sciatic nerve in adult male rats, but not any longer in senescent rats (Melcangi et al. 1999a).

It would be of interest to examine the effects of the progesterone derivates DHP and THP in future studies. Furthermore, other molecules that upregulate *Pmp22* expression or counteract the loss of *Pmp22* by targeting the receptors mentioned above, similar receptors or molecular pathways in HNPP mice are worth taking in consideration when planning a therapy study on the mouse model.

4.4. Conclusions

The aims set for the thesis: performing a comparison of the mouse model for HNPP to the limited amount of published data regarding its characteristics and further evaluating its similarity to human patients, as well as performing an expression study of *Pmp22* through pharmaceutical means with progesterone, were achieved in this study. In summary, apart from reproducing data obtained in previous studies with the mouse model, novel information on HNPP was gained. On the histological level, the presence of tomacula was reaffirmed and the number of tomacula and myelin invaginations was shown to increase with aging. The tomaculous formations were in line with findings in human HNPP patients. However, while the HNPP mice did not show a reduced number of axons, a decreased axon number is observed in patients. As for the electrophysiological findings, decreased NCVs were now for the first time observed in the mouse model. The electrophysiological characteristics of the mouse model mimic features in human patients with decreased CMAPs and NCVs and increased DMLs, and the presence of CB in a few HNPP mice reflects the situation in patients. It was demonstrated that the expression of *Pmp22* can be augmented with progesterone. Furthermore, the expression of *Krox-20* and *Pmp22* were shown to correlate to another, suggesting the role of KROX-20 as an inductor of *Pmp22* expression. The increased level of *Pmp22* expression, however, did not affect the pathological hallmarks of the HNPP mice.

The HNPP mouse model was shown to mimic pathological features of human patients to a certain extent, however as mentioned above, some issues remain to be resolved. Nevertheless, it can be concluded to serve as a valuable tool for future investigations. The results of this study can be seen as an excellent platform from which further experiments with progesterone can be performed, including optimization of the application form and the dosage, in order to determine its potential in counteracting the HNPP phenotype. Additionally, testing other substances and receptors able to stimulate *Pmp22* expression would be a logical step in the attempt to find a means to ameliorate the amount of *Pmp22* to wild type levels and thus potentially reach a normalization of the phenotype.

5. Summary

Hereditary neuropathy with liability to pressure palsies (HNPP) is an autosomal dominant demyelinating disorder characterized by episodic, recurrent peripheral sensory and motor neuropathies, triggered by minor traumas or compression in various locations. A typical clinical manifestation of HNPP is acute, painless, recurrent peripheral nerve palsies. The symptoms are brief and improve generally within days, weeks or months, with full recovery occurring in 50 % of episodes. The affected limbs usually show significant slowing and conduction blocks (CB) in nerve conduction velocity (NCV) studies, distal motor latencies (DML) are increased and sensory nerve conduction velocities are often decreased. In addition, sensory nerve action potential amplitudes are reduced. Only symptomatic treatment is currently available.

The majority of cases of HNPP can be attributed to a heterozygous 1.5 Mb deletion on chromosome 17p11.2 that includes the peripheral myelin protein 22 (*PMP22*) gene. PMP22 is an intrinsic membrane protein, primarily expressed in myelinating Schwann cells. PMP22 comprises approximately 2-5 % of total myelin protein and is largely confined to compact myelin. Its precise biological functions are still unknown but it has been proposed to serve as a structural component of myelin, required for the flawless development of peripheral nerves, axon maintenance, myelin formation and the determination of myelin thickness and stability.

The histological characteristics of HNPP nerves consist of focal excessive myelin folds (tomacula), characterized by an extremely thickened myelin sheath wrapping around an axon of reduced diameter, and onion bulbs. Tomacula may initially arise from myelin invaginations.

The signaling pathway of progesterone is known to regulate the mRNA expression of myelin genes in the peripheral nervous system. In the present study subcutaneous application of progesterone for a period of two months increased the *Pmp22* expression in the HNPP mice ($Pmp22^{+/-}$) to wild type levels. The expression of *Krox-20* and *Pmp22* correlated to one another, providing evidence for the role of KROX-20 as an inductor of *Pmp22* expression. Surprisingly, the effects of progesterone were not reflected on pathological myelin characteristics, which remained unchanged. This could be due to a possible threshold level that has to be reached for therapeutic effectiveness to occur. Tomacula and myelin invagi-

nations were shown to increase in number as the animals grew older. Reduced NCVs were detected in electrophysiological studies performed on the HNPP mice and earlier documented electrophysiological characteristics (decreased CMAPs and NCVs and increased DMLs) were reproduced. Even CBs were observed in a few HNPP mice. This mouse model was, albeit some limitations, shown to largely mimic the pathological features of human patients and can therefore be regarded as a valuable tool for future studies aiming to understand the disease mechanisms and could help lead to the development of new therapies.

6. References

Adlkofer K, Martini R, Aguzzi A, Zielasek J, Toyka KV, Suter U (1995): Hypermyelination and demyelinating peripheral neuropathy in Pmp22-deficient mice. Nat Genet 11, 274–280

Adlkofer K, Frei R, Neuberg DH, Zielasek J, Toyka KV, Suter U (1997): Heterozygous peripheral myelin protein 22-deficient mice are affected by a progressive demyelinating tomaculous neuropathy. J Neurosci 17, 4662–4671

Amato AA, Gronseth GS, Callerame KJ, Kagan-Hallet KS, Bryan WW, Barohn RJ (1996): Tomaculous neuropathy: a clinical and electrophysiological study in patients with and without 1.5-Mb deletions in chromosome 17p11.2. Muscle Nerve 19, 16–22

Amici SA, Dunn WA, Notterpek L (2007): Developmental abnormalities in the nerves of peripheral myelin protein 22-deficient mice. J Neurosci Res 85, 238–249

Attarian S, Vallat J-M, Magy L, Funalot B, Gonnaud P-M, Lacour A, Péréon Y, Dubourg O, Pouget J, Micallef J (2014): An exploratory randomised double-blind and placebo-controlled phase 2 study of a combination of baclofen, naltrexone and sorbitol (PXT3003) in patients with Charcot-Marie-Tooth disease type 1A. Orphanet J Rare Dis 2014 9, 199

Azcoitia I, Leonelli E, Magnaghi V, Veiga S, Garcia-Segura LM, Melcangi RC (2003): Progesterone and its derivatives dihydroprogesterone and tetrahydroprogesterone reduce myelin fiber morphological abnormalities and myelin fiber loss in the sciatic nerve of aged rats. Neurobiol Aging 24, 853-860

Bai Y, Zhang X, Katona I, Saporta MA, Shy ME, O'Malley HA, Isom LL, Suter U, Li J (2010): Conduction block in PMP22 deficiency. J Neurosci 30, 600–608

Baulieu EE (1997): Neurosteroids: of the nervous system, by the nervous system, for the nervous system. Recent Prog Horm Res 52, 1–32

Beato M (1989): Gene regulation by steroid hormones. Cell 56, 335–344

Behse F, Buchthal F, Carlsen F, Knappeis GG (1972a): Hereditary neuropathy with liability to pressure palsies. Electrophysiological and histopathological aspects. Brain 95, 777–794

Beydoun SR, Cho J (2013): Hereditary neuropathy with liability to pressure palsies: two cases of difficult diagnosis. J Clin Neuromusc Dis 15, 28-33

Bird TD: Hereditary Neuropathy with Liability to Pressure Palsies. [Updated 2014]. In: Pagon RA, Adam MP, Ardinger HH, Wallace SE, Amemiya A, Bean LJ, Bird TD, Fong C-T, Mefford HC, Smith RJ: GeneReviews®. Seattle (WA): University of Washington, Seattle 1993-2018

Bosse F, Zoidl G, Wilms S, Gillen CP, Kuhn HG, Müller HW (1994): Differential expression of two mRNA species indicates a dual function of peripheral myelin protein PMP22 in cell growth and myelination. J Neurosci Res 37, 529–537

Brockes JP, Raff MC, Nishiguchi DJ, Winter J (1980): Studies on cultured rat Schwann cells. III. Assays for peripheral myelin proteins. J Neurocytol 9, 67–77

Caruso D, Scurati S, Roglio I, Nobbio L, Schenone A, Melcangi RC (2008): Neuroactive steroid levels in a transgenic rat model of CMT1A neuropathy. J Mol Neurosci 34, 249-253

Celotti F, Melcangi RC, Martini L (1992): The 5 alpha-reductase in the brain: molecular aspects and relation to brain function. Front Neuroendocrinol 13, 163-215

Chabbert-Buffet N, Meduri G, Bouchard P, Spitz IM (2005): Selective progesterone receptor modulators and progesterone antagonists: mechanisms of action and clinical applications. Hum Reprod Update 11, 293-307

Chan JR, Phillips LJ, Glaser M (1998): Glucocorticoids and progestins signal the initiation and enhance the rate of myelin formation. Proc Natl Acad Sci U S A 95, 10459–10464

Chance PF, Fischbeck KH (1994): Molecular genetics of Charcot-Marie-Tooth disease and related neuropathies. Hum Mol Genet 3 Spec No, 1503–1507

Chance PF, Alderson MK, Leppig KA, Lensch MW, Matsunami N, Smith B, Swanson PD, Odelberg SJ, Disteche CM, Bird TD (1993): DNA deletion associated with hereditary neuropathy with liability to pressure palsies. Cell 72, 143–151

Chittoor-Vinod VG, Lee S, Judge SM, Notterpek L (2015): Inducible HSP70 is critical in preventing the aggregation and enhancing the processing of PMP22. ASN Neuro 7

Chumakov I, Milet A, Cholet N, Primas G, Boucard A, Pereira Y, Graudens E, Mandel J, Laffaire J, Foucquier J (2014): Polytherapy with a combination of three repurposed drugs (PXT3003) down-regulates Pmp22 over-expression and improves myelination, axonal and functional parameters in models of CMT1A neuropathy. Orphanet J Rare Dis 9, 201

Cho S-M, Hong BY, Kim Y, Lee SG, Yang J-Y, Kim J, Lee K-A (2014): Partial Gene Deletions of PMP22 Causing Hereditary Neuropathy with Liability to Pressure Palsies. Case Rep Genet 2014, 946010

Cruz-Martinez A, Arpa J, Palau F (2000): Peroneal neuropathy after weight loss. J Peripher Nerv Syst 5, 101–105

Davies DM (1954): Recurrent peripheral nerve palsies in a family. Lancet 267, 266–268

De Jong JGY (1947): Over families met hereditaire dispositie tot het optreden van neuritiden, gecorreleerd met migraine. Monatsschr Psychiatr Neurol 50, 60–76

De Oliveira APM, Pereira RC, Onofre PT, Marques VD, de Andrade GB, Barreira AA, Marques JW (2016): Clinical and neurophysical features of the hereditary neuropathy with liability to pressure palsy due to the 17p11.2 deletion. Arq Neuropsiquiatr 74, 99-105

Decker L, Desmarquet-Trin-Dinh C, Taillebourg E, Ghislain J, Vallat J-M, Charnay P (2006): Peripheral myelin maintenance is a dynamic process requiring constant Krox20 expression. J Neurosci 26, 9771–9779

Del Colle R, Fabrizi GM, Turazzini M, Cavallaro T, Silvestri M, Rizzuto N (2003): Hereditary neuropathy with liability to pressure palsies: electrophysiological and genetic study of a family with carpal tunnel syndrome as only clinical manifestation. Neurol Sci 24, 57–60

Désarnaud F, Do Thi AN, Brown AM, Lemke G, Suter U, Baulieu EE, Schumacher M (1998): Progesterone stimulates the activity of the promoters of peripheral myelin protein-22 and protein zero genes in Schwann cells. J Neurochem 71, 1765–1768

Dubourg O, Mouton P, Brice A, LeGuern E, Bouche P (2000): Guidelines for diagnosis of hereditary neuropathy with liability to pressure palsies. Neuromuscul Disord 10, 206-208

D'Urso D, Ehrhardt P, Müller HW (1999): Peripheral myelin protein 22 and protein zero: a novel association in peripheral nervous system myelin. J Neurosci 19, 3396–3403

Dyck P, Thomas PK: Peripheral neuropathy. 4th edition; Saunders, Philadelphia 2005

Earl CJ, Fullerton PM, Wakefield GS, Schutta HS (1964): Hereditary neuropathy, with liability to pressure palsies; a clinical and electrophysiological study of four families. Q J Med 33, 481–498

Earle N, Zochodne D (2013): Is carpal tunnel decompression warranted for HNPP? J Peripher Nerv Syst 18, 331-335

Ekins S, Litterman NK, Arnold RJG, Burgess RW, Freundlich JS, Gray SJ, Higgins JJ, Langley B, Willis DE, Notterpek L (2015): A brief review of recent Charcot-Marie-Tooth research and priorities. F1000Res 4, 53

Emery AE (1991): Population frequencies of inherited neuromuscular diseases--a world survey. Neuromuscul Disord 1, 19–29

Farrar MA, Park SB, Krishnan AV, Kiernan MC, Lin CS-Y (2014): Axonal dysfunction, dysmyelination, and conduction failure in hereditary neuropathy with liability to pressure palsies. Muscle Nerve 49, 858-865

Fawcett JW, Keynes RJ (1990): Peripheral nerve regeneration. Annu Rev Neurosci 13, 43–60

Fledrich R, Stassart R, Klink A, Rasch LM, Prukop T, Haag L, Czesnik D, Kungl T, Abdelaal TAM, Keric N (2014): Soluble neuregulin-1 modulates disease pathogenesis in rodent models of Charcot-Marie-Tooth disease 1A. Nat Med 20, 1055-1061

Giatti S, Romano S, Pesaresi M, Cermenati G, Mitro N, Caruso D, Tetel MJ, Garcia-Segura LM, Melcangi RC (2015): Neuroactive steroids and the peripheral nervous system: An update. Steroids 103, 23–30

Gouider R, LeGuern E, Gugenheim M, Tardieu S, Maisonobe T, Léger JM, Vallat JM, Agid Y, Bouche P, Brice A (1995): Clinical, electrophysiologic and molecular correlations in 13 families with hereditary neuropathy with liability to pressure palsies and a chromosome 17p11.2 deletion. Neurology 45, 2018-2023

Guennoun R, Benmessahel Y, Delespierre B, Gouézou M, Rajkowski KM, Baulieu EE, Schumacher M (2001): Progesterone stimulates Krox-20 gene expression in Schwann cells. Brain Res Mol Brain Res 90, 75–82

Guo J, Wang L, Zhang Y, Wu J, Arpag S, Hu B, Imhof BA, Tian X, Carter BD, Suter U (2014): Abnormal junctions and permeability of myelin in PMP22-deficient nerves. Ann Neurol 75, 255–265

Hellemans J, Mortier G, De Paepe A, Speleman F, Vandesompele J (2007): qBase relative quantification framework and software for management and automated analysis of real-time quantitative PCR data. Genome Biol 8, R19

Herskovitz S, Scelsa S, Schaumburg H: Peripheral neuropathies in clinical practice. Oxford University Press, Oxford 2010

Hong Y-H, Kim M, Kim H-J, Sung J-J, Kim SH, Lee K-W (2003): Clinical and electrophysiologic features of HNPP patients with 17p11.2 deletion. Acta Neurol Scand 108, 352–358

Hu B, Arpag S, Zhang X, Möbius W, Werner H, Sosinsky G, Ellisman M, Zhang Y, Hamilton A, Chernoff J (2016): Tuning PAK activity to rescue abnormal myelin permeability in HNPP. PLoS Genet 12, e1006290

Infante J, García A, Combarros O, Mateo JI, Berciano J, Sedano MJ, Gutiérrez-Rivas EJ, Palau F (2001): Diagnostic strategy for familial and sporadic cases of neuropathy associated with 17p11.2 deletion. Muscle Nerve 24, 1149-1155

Inglese J, Dranchak P, Moran JJ, Jang S-W, Srinivasan R, Santiago Y, Zhang L, Guha R, Martinez N, MacArthur R (2014): Genome editing-enabled HTS assays expand drug target pathways for Charcot-Marie-Tooth disease. ACS Chem Biol 9, 2594-2602

Ishaque A, Roomi MW, Szymanska I, Kowalski S, Eylar EH (1980): The PO glycoprotein of peripheral nerve myelin. Can J Biochem 58, 913–921

Jacobsen BM, Horwitz KB (2012): Progesterone receptors, their isoforms and progesterone regulated transcription. Mol Cell Endocrinol 357, 18–29

Jacobsen BM, Jambal P, Schittone SA, Horwitz KB (2009): ALU Repeats in Promoters Are Position-Dependent Co-Response Elements (coRE) that Enhance or Repress Transcription by Dimeric and Monomeric Progesterone Receptors. Mol Endocrinol 23, 989–1000

Jankelowitz SK, Burke D (2013): Pathophysiology of HNPP explored using axonal excitability. J Neurol Neurosurg Psychiatr 84, 806–812

Jetten AM, Suter U (2000): The peripheral myelin protein 22 and epithelial membrane protein family. Prog Nucleic Acid Res Mol Biol 64, 97–129

Jung-Testas I, Schumacher M, Robel P, Baulieu EE (1996): Demonstration of progesterone receptors in rat Schwann cells. J Steroid Biochem Mol Biol 58, 77–82

Kaji R (2003): Physiology of conduction block in multifocal motor neuropathy and other demyelinating neuropathies. Muscle Nerve 27, 285-96

Kalfakis N, Panas M, Karadima G, Floroskufi P, Kokolakis N, Vassilopoulos D (2002): Hereditary neuropathy with liability to pressure palsies emerging during vincristine treatment. Neurology 59, 1470–1471

Karlsson, U, Schultz, RL (1965): Fixation of the central nervous system from electron microscopy by aldehyde perfusion. J Ultrastruct Res 12, 160-186

Koenig HL, Schumacher M, Ferzaz B, Thi AN, Ressouches A, Guennoun R, Jung-Testas I, Robel P, Akwa Y, Baulieu EE (1995): Progesterone synthesis and myelin formation by Schwann cells. Science 268, 1500–1503

Koike H, Hirayama M, Yamamoto M, Ito H, Hattori N, Umehara F, Arimura K, Ikeda S, Ando Y, Nakazato M (2005): Age associated axonal features in HNPP with 17p11.2 deletion in Japan. J Neurol Neurosurg Psychiatr 76, 1109-11014

Kramer M, Ly A, Li J (2016): Phenotype HNPP (Hereditary Neuropathy with Liability to Pressure Palsies) induced by medical procedures. Am J Orthop 45, E27-E28

Lawson VH, Arnold WD (2014): Multifocal motor neuropathy: a review of pathogenesis, diagnosis, and treatment. Neuropsychiatr Dis Treat 10, 567-76

Le N, Nagarajan R, Wang JYT, Araki T, Schmidt RE, Milbrandt J (2005): Analysis of congenital hypomyelinating Egr2Lo/Lo nerves identifies Sox2 as an inhibitor of Schwann cell differentiation and myelination. Proc Natl Acad Sci U S A 102, 2596–2601

Lee S, Amici S, Tavori H, Zeng W, Freeland S, Fazio S, Notterpek L (2014): PMP22 is critical for actin-mediated cellular functions and for establishing lipid rafts. J Neurosci 48, 16140-16152

Lenssen PP, Gabreëls-Festen AA, Valentijn LJ, Jongen PJ, van Beersum SE, van Engelen BG, van Wensen PJ, Bolhuis PA, Gabreëls FJ, Mariman EC (1998): Hereditary neuropathy with liability to pressure palsies. Phenotypic differences between patients with the common deletion and a PMP22 frame shift mutation. Brain 121, 1451-1458

Li J, Krajewski K, Shy ME, Lewis RA (2002): Hereditary neuropathy with liability to pressure palsy: the electrophysiology fits the name. Neurology 58, 1769–1773

Li J, Krajewski K, Lewis RA, Shy ME (2004): Loss-of-function phenotype of hereditary neuropathy with liability to pressure palsies. Muscle Nerve 29, 205–210

Li J, Parker B, Martyn C, Natarajan C, Guo J (2013): The PMP22 gene and its related diseases. Mol Neurobiol 47, 673–698

Luft JH (1961): Improvements in epoxy resin embedding methods. J Biophys Biochem Cytol 9, 409-414

Luigetti M, Del Grande A, Conte A, Lo Monaco M, Bisogni G, Romano A, Zollino M, Rossini PM, Sabatelli M (2014): Clinical, neurohysiological and pathological findings of HNPP patients with 17p12 deletion: a single-centre experience. J Neurol Sci 341, 46-50

Lupski JR, de Oca-Luna RM, Slaugenhaupt S, Pentao L, Guzzetta V, Trask BJ, Saucedo-Cardenas O, Barker DF, Killian JM, Garcia CA (1991): DNA duplication associated with Charcot-Marie-Tooth disease type 1A. Cell 66, 219–232

Madrid R and Bradley WG (1975): The pathology of neuropathies with focal thickening of the myelin sheath (tomaculous neuropathy). J Neurol Sci 25, 415-448

Magnaghi V, Ballabio M, Roglio I, Melcangi RC (2007): Progesterone derivatives increase expression of Krox-20 and Sox-10 in rat Schwann cells. J Mol Neurosci MN 31, 149–157

Marriott M, Macdonell R, McCrory P (2002): Flail arms in a parachutist: an unusual presentation of hereditary neuropathy with liability to pressure palsies. Br J Sports Med 36, 465–466

Martini L, Magnaghi V, Melcangi RC (2003): Actions of progesterone and its 5alpha-reduced metabolites on the major proteins of the myelin of the peripheral nervous system. Steroids 68, 825–829

Martini R, Schachner M (1997): Molecular bases of myelin formation as revealed by investigations on mice deficient in glial cell surface molecules. Glia 19, 298–310

McKenna NJ, O'Malley BW (2002): Combinatorial control of gene expression by nuclear receptors and coregulators. Cell 108, 465–474

Melcangi RC, Celotti F, Ballabio M, Poletti A, Martini L (1990): Testosterone metabolism in peripheral nerves: presence of the 5 alpha-reductase-3 alpha-hydroxysteroid-dehydrogenase enzymatic system in the sciatic nerve of adult and aged rats. J Steroid Biochem 35, 145-148

Melcangi RC, Poletti A, Cavarretta I, Celotti F, Colciago A, Magnaghi V, Motta M, Negri-Cesi P, Martini L (1998a): The 5alpha-reductase in the central nervous system: expression and modes of control. J Steroid Biochem Mol Biol 65, 295-299

Melcangi RC, Magnaghi V, Cavarretta I, Martini L, Piva F (1998b): Age-induced decrease of glycoprotein Po and myelin basic protein gene expression in the rat sciatic nerve. Repair by steroid derivates. Neuroscience 85, 569-578

Melcangi RC, Magnaghi V, Cavarretta I, Zucchi I, Bovolin P, D'Urso D, Martini L (1999a): Progesterone derivatives are able to influence peripheral myelin protein 22 and P0 gene expression: possible mechanisms of action. J Neurosci Res 56, 349–357

Melcangi RC, Magnaghi V, Martini L (1999b): Steroid metabolism and effects in central and peripheral glial cells. J Neurobiol 40, 471-483

Melcangi RC, Magnaghi V, Galbiati M, Martini L (2001): Formation and effects of neuroactive steroids in the central and peripheral nervous system. Int Rev Neurobiol 46, 145-176

Melcangi RC, Azcoitia I, Ballabio M, Cavarretta I, Gonzalez LC, Leonelli E, Magnaghi V, Veiga S, Garcia-Segura LM (2003): Neuroactive steroids influence peripheral myelination: a promising opportunity for preventing or treating age-dependent dysfunctions of peripheral nerves. Prog Neurobiol 71, 57-66

Melcangi RC, Cavarretta ITR, Ballabio M, Leonelli E, Schenone A, Azcoitia I, Miguel Garcia-Segura L, Magnaghi V (2005): Peripheral nerves: a target for the action of neuroactive steroids. Brain Res Brain Res Rev 48, 328-338

Mercier G, Turque N, Schumacher M (2001): Early activation of transcription factor expression in Schwann cells by progesterone. Brain Res Mol Brain Res 97, 137–148

Meretoja P, Silander K, Kalimo H, Aula P, Meretoja A, Savontaus ML (1997): Epidemiology of hereditary neuropathy with liability to pressure palsies (HNPP) in south western Finland. Neuromuscul Disord 7, 529–532

Meyer zu Hörste G, Prukop T, Nave K-A, Sereda MW (2006): Myelin disorders: Causes and perspectives of Charcot-Marie-Tooth neuropathy. J Mol Neurosci MN 28, 77–88

Meyer zu Hörste G, Prukop T, Liebetanz D, Mobius W, Nave K-A, Sereda MW (2007): Antiprogesterone therapy uncouples axonal loss from demyelination in a transgenic rat model of CMT1A neuropathy. Ann Neurol 61, 61-72

Morrison TB, Weis JJ, Wittwer CT (1998): Quantification of low-copy transcripts by continuous SYBR Green I monitoring during amplification. Biotechniques 24, 954-962

Mouton P, Tardieu S, Gouider R, Birouk N, Maisonobe T, Dubourg O, Brice A, LeGuern E, Bouche P (1999): Spectrum of clinical and electrophysiologic features in HNPP patients with the 17p11.2 deletion. Neurology 52, 1440-1446

Mullis K, Faloona F, Scharf S, Saiki R, Horn G, Erlich H (1986): Specific enzymatic amplification of DNA in vitro: the polymerase chain reaction. Biotechnology 24, 17-27

Murphy P, Topilko P, Schneider-Maunoury S, Seitanidou T, Baron-Van Evercooren A, Charnay P (1996): The regulation of Krox-20 expression reveals important steps in the control of peripheral glial cell development. Development 122, 2847–2857

Nagarajan R, Svaren J, Le N, Araki T, Watson M, Milbrandt J (2001): EGR2 mutations in inherited neuropathies dominant-negatively inhibit myelin gene expression. Neuron 30, 355–368

Nicholson GA, Valentijn LJ, Cherryson AK, Kennerson ML, Bragg TL, DeKroon RM, Ross DA, Pollard JD, McLeod JG, Bolhuis PA (1994): A frame shift mutation in the PMP22 gene in hereditary neuropathy with liability to pressure palsies. Nat Genet 6, 263–266

Nordborg C, Conradi N, Sourander P, Hagberg B, Westerberg B (1984): Hereditary motor and sensory neuropathy of demyelinating and remyelinating type in children. Ultrastructural and morphometric studies on sural nerve biopsy specimens from ten sporadic cases. Acta Neuropathol 65, 1–9

Notterpek L, Snipes GJ, Shooter EM (1999): Temporal expression pattern of peripheral myelin protein 22 during in vivo and in vitro myelination. Glia 25, 358–369

Oda K, Miura H, Shibasaki H, Endo C, Kakigi R, Kuroda Y, Tanaka K (1990): Hereditary pressure-sensitive neuropathy: demonstration of „tomacula“ in motor nerve fibers. J Neurol Sci 98, 139–148

Pareek S, Suter U, Snipes GJ, Welcher AA, Shooter EM, Murphy RA (1993): Detection and processing of peripheral myelin protein PMP22 in cultured Schwann cells. J Biol Chem 268, 10372–10379

Pareyson D, Scaioli V, Taroni F, Botti S, Lorenzetti D, Solari A, Ciano C, Sghirlanzoni A (1996): Phenotypic heterogeneity in hereditary neuropathy with liability to pressure palsies associated with chromosome 17p11.2-12 deletion. Neurology 46, 1133–1137

Perrin S (2014): Preclinical research: Make mouse studies work. Nature 507, 423-425

Pou Serradell A, Monells J, Téllez MJ, Fossas P, Löfgren A, Meuleman J, Timmerman V, De Jonghe P, Ceuterick C, Martin JJ (2002): [Hereditary neuropathy with liability to pressure palsies: study of six Spanish families]. Rev Neurol (Paris) 158: 579-588

Prukop T: Tierexperimentelle Studien zur Behandlung der axonalen Degeneration bei primär glialen Gendosisdefekten des zentralen und peripheren Nervensystems. Med. Diss. Göttingen 2008

Prukop T, Wernick S, Adam J, Zschüntzsch J, Schmidt J, Brureau A, Foucquier J, Guedj M, Cholet N, Nave K-A (2017): The combinational drug PXT3003 improves neuromuscular function in an animal model of Charcot-Marie-Tooth type 1A disease. 2017 PNS Annual Meeting, Sitges, Spain, 8-12 July 2017

Quarles RH (1997): Glycoproteins of myelin sheaths. J Mol Neurosci 8, 1–12

Richardson KC, Jarett L, Finke EH (1960): Embedding in epoxy resins for ultrathin sectioning in electron microscopy. Stain Technol 35, 313-323

Rossor AM, Evans MRB, Reilly MM (2015): A practical approach to the genetic neuropathies. Pract Neurol 15, 187-198

Rossor AM, Tomaselli PJ, Reilly MM (2016): Recent advances in the genetic neuropathies. Curr Opin Neurol 29, 537-548

Ruan B-F, Zhu H-L (2012): The chemistry and biology of the bryostatins: potential PKC inhibitors in clinical development. Curr Med Chem 19, 2652-2664

Rupprecht R, Reul JM, Trapp T, van Steensel B, Wetzel C, Damm K, Zieglgänsberger W, Holsboer F (1993): Progesterone receptor-mediated effects of neuroactive steroids. Neuron 11, 523-530

Rupprecht R, Hauser CA, Trapp T, Holsboer F (1996): Neurosteroids: molecular mechanisms of action and psychopharmacological significance. J Steroid Biochem Mol Biol 56, 163-168

Sander S, Ouvrier RA, McLeod JG, Nicholson GA, Pollard JD (2000): Clinical syndromes associated with tomacula or myelin swellings in sural nerve biopsies. J Neurol Neurosurg Psychiatr 68, 483–488

Schenone A: Principles of pathology and nerve biopsy. In: Kuhlenbäumer G, Stögbauer F, Ringelstein EB, Young P: Hereditary peripheral neuropathies. Steinkopff-Verlag, Darmstadt 2005, 41-72

Schumacher M, Guennoun R, Mercier G, Désarnaud F, Lacor P, Bénavides J, Ferzaz B, Robert F, Baulieu EE (2001): Progesterone synthesis and myelin formation in peripheral nerves. Brain Res Brain Res Rev 37, 343–359

Schumacher M, Hussain R, Gago N, Oudinet J-P, Mattern C, Ghoumari AM (2012): Progesterone synthesis in the nervous system: implications for myelination and myelin repair. Front Neurosci 6, 10

Sereda MW, Nave K-A (2006): Animal models of Charcot-Marie-Tooth disease type 1A. Neuromolecular Med 8, 205–216

Sereda MW, Meyer zu Hörste G, Suter U, Uzma N, Nave K-A (2003): Therapeutic administration of progesterone antagonist in a model of Charcot-Marie-Tooth disease (CMT-1A). Nat Med 9, 1533–1537

Snipes GJ, Suter U, Welcher AA, Shooter EM (1992): Characterization of a novel peripheral nervous system myelin protein (PMP-22/SR13). J Cell Biol 117, 225–238

Staal A, de Weerdt CJ, Went LN (1965): Hereditary compression syndrome of peripheral nerves. Neurology 15, 1008–1017

Stögbauer F, Young P, Kuhlenbäumer G, De Jonghe P, Timmerman V (2000): Hereditary recurrent focal neuropathies: clinical and molecular features. Neurology 54, 546–551

Stoll G, Müller HW (1999): Nerve injury, axonal degeneration and neural regeneration: basic insights. Brain Pathol 9, 313–325

Suter U, Nave K-A (1999): Transgenic mouse models of CMT1A and HNPP. Ann N Y Acad Sci 883, 247–253

Suter U, Snipes GJ (1995a): Biology and genetics of hereditary motor and sensory neuropathies. Annu Rev Neurosci 18, 45–75

Suter U, Snipes GJ (1995b): Peripheral myelin protein 22: facts and hypotheses. J Neurosci Res 40, 145–151

Suter U, Welcher AA, Ozcelik T, Snipes GJ, Kosaras B, Francke U, Billings-Gagliardi S, Sidman RL, Shooter EM (1992): Trembler mouse carries a point mutation in a myelin gene. Nature 356, 241–244

Suter U, Snipes GJ, Schoener-Scott R, Welcher AA, Pareek S, Lupski JR, Murphy RA, Shooter EM, Patel PI (1994): Regulation of tissue-specific expression of alternative peripheral myelin protein-22 (PMP22) gene transcripts by two promoters. J Biol Chem 269, 25795–25808

Thomas FP, Lebo RV, Rosoklija G, Ding XS, Lovelace RE, Latov N, Hays AP (1994): Tomaculous neuropathy in chromosome 1 Charcot-Marie-Tooth syndrome. Acta Neuropathol 87, 91–97

Topilko P, Schneider-Maunoury S, Levi G, Baron-Van Evercooren A, Chennoufi AB, Seitanidou T, Babinet C, Charnay P (1994): Krox-20 controls myelination in the peripheral nervous system. Nature 371, 796–799

Van Paassen BW, van der Kooi AJ, van Spaendonck-Zwarts KY, Verhamme C, Baas F, de Visser M (2014): PMP22 related neuropathies: Charcot-Marie-Tooth disease type 1A and Hereditary Neuropathy with liability to Pressure Palsies. Orphanet J Rare Dis 9, 38

Vandesompele J, De Preter K, Pattyn F, Poppe B, Van Roy N, De Paepe A, Speleman F (2002): Accurate normalization of real-time quantitative RT-PCR data by geometric averaging of multiple internal control genes. Genome Biol 3, Research0034

Vital C, Pautrizel B, Lagueny A, Vital A, Bergouignan FX, David B, Loiseau P (1985): [Hypermyelination in a case of peripheral neuropathy with benign IgM monoclonal gammopathy]. Rev Neurol (Paris) 141, 729–734

Windebank AJ: Inherited recurrent focal neuropathies. In: Dyck PJ, Thomas PK, Griffin JW, Low PA, Poduslo JF, eds.: Peripheral neuropathy. 3rd edition; Saunders, Philadelphia 1993, 1137-1148

Welcher AA, Suter U, De Leon M, Snipes GJ, Shooter EM (1991): A myelin protein is encoded by the homologue of a growth arrest-specific gene. Proc Natl Acad Sci U S A 88, 7195–7199

Wu R-C, Smith CL, O'Malley BW (2005): Transcriptional regulation by steroid receptor coactivator phosphorylation. Endocr Rev 26, 393–399

Yokoi H, Tsuruo Y, Ishimura K (1998): Steroid 5alpha-reductase type 1 immunolocalized in the rat peripheral nervous system and paraganglia. Histochem J 30, 731-739

Yurrebaso I, Casado OL, Barcena J, Perez de Nanclares G, Aguirre U (2014): Clinical, electrophysiological and magnetic resonance findings in a family with hereditary neuropathy with liability to pressure palsies caused by a novel PMP22 mutation. Neuromuscul Disord 24, 56-62

Zhu J, Chen W, Mi R, Zhou C, Reed N, Höke A (2013): Ethoxyquin prevents chemotherapy-induced neurotoxicity via Hsp90 modulation. Ann Neurol 74, 893-904

Zorick TS, Syroid DE, Arroyo E, Scherer SS, Lemke G (1996): The Transcription Factors SCIP and Krox-20 Mark Distinct Stages and Cell Fates in Schwann Cell Differentiation. Mol Cell Neurosci 8, 129–145

Zorick TS, Syroid DE, Brown A, Gridley T, Lemke G (1999): Krox-20 controls SCIP expression, cell cycle exit and susceptibility to apoptosis in developing myelinating Schwann cells. Development 126, 1397–1406

Acknowledgements

I would like to thank Prof. Dr. med. Michael Sereda (Max-Planck Institute for Experimental Medicine, Göttingen) for giving me the possibility to work in his research group.

My sincere gratitude goes to Dr. med. Ruth Stassart and Dr. Robert Fledrich for their valuable advice and guidance during my research work and their immense knowledge. I also thank Dr. Robert Fledrich for his help with the electrophysiological measurements.

I am most grateful to Dr. med. Thomas Prukop for his patient guidance, useful critiques and invaluable help during my process of writing the thesis.

I would like to express my sincere gratitude to Dr. Theresa Kungl, Dr. Liam Tuffy, Torben Ruhwedel and Carolin Böhler, as well as to all the other kind and helpful colleagues at Max-Planck Institute of Experimental Medicine, for technical advice and interesting scientific discussions.

I thank Prof. Dr. Kathrin Adlkofer, Prof. Dr. Florian Stögbauer, Prof. Dr. John Pollard and Dr. med. Gerd Meyer zu Hörste for their kind permission to use their published figures in my thesis. I also thank the publishers for the permission; Wolters Kluwer Health, Inc., BMJ Publishing Group Ltd., Society for Neuroscience and Springer Nature.